

AD-A248 083



2

NAVAL POSTGRADUATE SCHOOL

Monterey, California



THESIS

TWO - DIMENSIONAL BOUNDARY SURFACES
FOR
PLANAR EXTERNAL TRANSONIC FLOWS

by

Aharon Salama

MARCH, 1992

Thesis Advisor:

O. Biblarz

Approved for public release; distribution is unlimited

*Original contains color
plates: All DTIC reproductions
will be in black and
white

92-07841



92 3 27 027

REPORT DOCUMENTATION PAGE			
1a REPORT SECURITY CLASSIFICATION Unclassified		1b RESTRICTIVE MARKINGS	
2a SECURITY CLASSIFICATION AUTHORITY		3 DISTRIBUTION/AVAILABILITY OF REPORT Approved for public release; distribution is unlimited	
2b DECLASSIFICATION/DOWNGRADING SCHEDULE			
4 PERFORMING ORGANIZATION REPORT NUMBER(S)		5. MONITORING ORGANIZATION REPORT NUMBER(S)	
6a NAME OF PERFORMING ORGANIZATION Naval Postgraduate School	5b OFFICE SYMBOL (If applicable) AA	7a NAME OF MONITORING ORGANIZATION Naval Postgraduate School	
6c. ADDRESS (City, State, and ZIP Code) Monterey, CA 93943-5000		7b. ADDRESS (City, State, and ZIP Code) Monterey, CA 93943-5000	
8a NAME OF FUNDING/SPONSORING ORGANIZATION	8b OFFICE SYMBOL (If applicable)	9 PROCUREMENT INSTRUMENT IDENTIFICATION NUMBER	
8c ADDRESS (City, State, and ZIP Code)		10 SOURCE OF FUNDING NUMBERS	
		Program Element No.	Project No.
		Task No.	Work Unit or Subproject Name
11 TITLE (Include Security Classification) TWO-DIMENSIONAL BOUNDARY SURFACES FOR PLANAR EXTERNAL TRANSONIC FLOWS.			
12 PERSONAL AUTHOR(S) AHARON SALAMA			
13a TYPE OF REPORT Master's Thesis	13b TIME COVERED From To	14 DATE OF REPORT (year, month, day) MARCH 1992	15 PAGE COUNT 67
16 SUPPLEMENTARY NOTATION The views expressed in this thesis are those of the author and do not reflect the official policy or position of the Department of Defense or the U.S. Government.			
17 COSATI CODES		18 SUBJECT TERMS (continue on reverse if necessary and identify by block number)	
FIELD	GROUP	SUBGROUP	
19 ABSTRACT (continue on reverse if necessary and identify by block number) The small perturbation, two dimensional transonic equation is manipulated with a separation of variables approach to obtain two ordinary, nonlinear differential equations. Numerical integration of these differential equations results in new transonic boundary surfaces for planar external flows. A key ingredient in these solutions is the identification of dependence of two integration constants, alpha and beta, on the parameter ($1 - M^2$). The anticipated behavior for both Mach number and the pressure coefficient is used as a guide in the actual selection of the adjustable constants in the problem. The physical reality of the boundary surfaces is examined by displaying the boundary conditions they satisfy. The strictly sonic flow ($Mach = 1.0$) has an analytic representation corresponding to a divergent surface which goes supersonic. The sonic solution is compared with an Euler-CFD approach confirming the validity of our results over the region where small perturbations apply. Solutions are also shown for $Mach = 0.8, 0.9, 1.1$ and 1.2 . These results are consistent with known behavior for both subsonic and supersonic external flows. Since the results of this work yield actual transonic contours, we can examine shockless surfaces for design applications. The possibility of starting with transonic surface is of interest to present day CFD approach. Finally an entire transonic upper surface is presented for $Mach = 0.8$, by patching a subsonic Mach number, which reaches a plateau at $M = 1.0$, with sonic flow. This patching requires the careful interpretation of a nondimensional reference length, called Y_0 , which is a function of Mach number.			
20 DISTRIBUTION/AVAILABILITY OF ABSTRACT <input checked="" type="checkbox"/> UNCLASSIFIED UNLIMITED <input type="checkbox"/> SAME AS REPORT <input type="checkbox"/> DTIC USERS		21 ABSTRACT SECURITY CLASSIFICATION Unclassified	
22a NAME OF RESPONSIBLE INDIVIDUAL (1) Biblarz		22b TELEPHONE (Include Area code) (408) 646 3096	22c OFFICE SYMBOL AA/B1

Approved for public release; distribution is unlimited.

Two Dimensional Boundary Surfaces
for
Planar External Transonic Flows

by

Aharon Salama
Major, Israeli Air Force

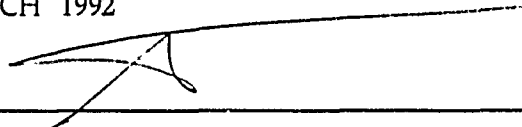
Submitted in partial fulfillment
of the requirements for the degree of

MASTER OF SCIENCE
IN AERONAUTICAL ENGINEERING

from the

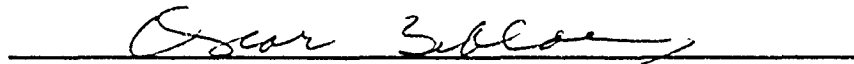
NAVAL POSTGRADUATE SCHOOL
MARCH 1992

Author:

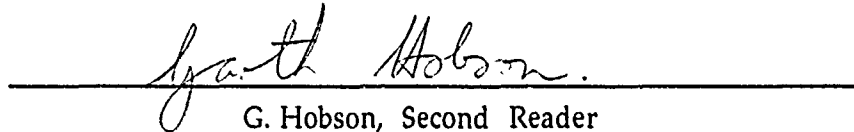


Aharon Salama

Approved by:



O. Biblarz, Thesis Advisor



G. Hobson, Second Reader



D. J. Collins, Chairman

Department of Aeronautical Engineering

ABSTRACT

The small perturbation, two-dimensional transonic equation is manipulated with a separation-of-variables approach to obtain two ordinary, nonlinear, differential equations. Numerical integration of these differential equations results in new transonic boundary surfaces for planar external flows. A key ingredient in these solutions is the identification of dependence of two integrations constants, α and β , on the parameter $(1-M_\infty^2)$. The anticipated behavior for both the Mach number and the pressure coefficient is used as a guide in the actual selection of the adjustable constants in the problem. The physical reality of our boundary surfaces is examined by displaying the boundary conditions they satisfy. The strictly sonic flow ($M_\infty=1.0$) has an analytic representation corresponding to a divergent surface which goes supersonic. This sonic solution is compared with an Euler-CFD approach confirming the validity of our results over the region where small perturbations apply. Solutions are also shown for $M_\infty=0.8, 0.9, 1.1$, and 1.2 . These results are consistent with known behavior for both subsonic and supersonic external flow. Since the results of this work yield actual transonic contours, we can examine shockless surfaces for design applications. The possibility of starting with transonic surface is of interest to present day CFD approach. Finally an entire transonic upper surface is presented for $M_\infty=0.8$, by patching a subsonic Mach number, which reaches a plateau at $M=1.0$, with a sonic flow. This patching requires the careful interpretation of a nondimensional reference length, called Y_0 , which is a function of M_∞ .

TABLE OF CONTENTS

I.	INTRODUCTION	1
II.	THE TRANSONIC EQUATION	3
III.	THE GOVERNING DIFFERENTIAL EQUATIONS	5
IV.	NUMERICAL INTEGRATION	11
V.	BOUNDARY SURFACES	15
VI.	PRESSURE COEFFICIENT	21
VII.	THE LOCAL MACH NUMBER	23
VIII.	BOUNDARY CONDITIONS	25
IX.	CONCLUSIONS	31
	LIST OF REFERENCES	32
	APPENDIX A: COMPUTER PROGRAMS	33
	APPENDIX B: FORM OF α AND β	37
	APPENDIX C: FIGURES	39
	INITIAL DISTRIBUTION LIST	60

ACKNOWLEDGEMENTS

I wish to express my thanks and deep appreciation to Prof. O. Biblarz for his continued guidance and support through the preparation of this research. I would also like to acknowledge the comments and suggestions made by Prof. G. Hobson on his CFD instruction. Special thanks to my commanders in the Israeli Air Force who made this moment possible for me. Finally, I am indebted to my wife, Edna, for her encouragement and patience.



Accession For	
NTIS GRA&I	<input checked="checked" type="checkbox"/>
DTIC TAB	<input type="checkbox"/>
Unannounced	<input type="checkbox"/>
Justification	
By	
Distribution/	
Availability Codes	
Dist	Avail and/or Special
A-1	

I. INTRODUCTION

The governing nonlinear equations, together with realistic boundary conditions have always been the main difficulty in transonic aerodynamic analysis, [Ref. 1]. While the hodograph transformations approach linearizes these equations, the transformations are confined to a limited number of transonic flows due to complicated boundary conditions. The small perturbation approach simplifies the full potential Equations; furthermore, like other predictive methods, it succeeds in retaining the great sensitivity of transonic flows within small perturbations. This paper expands on the exact solution of the small perturbation, nonlinear, two dimensional, transonic equation, using the guidelines and tools given by Biblarz O., [Refs. 2 and 3]. Starting with a separation-of-variables approach, Chap. III reveals two nonlinear, ordinary, differential equations which lead into two exact solutions. Chaps. IV and V describe the numerical integration of these implicit solutions, which finally yield the boundary surfaces. Later, these boundary surfaces are found to satisfy the boundary conditions for a two dimensional surfaces. These findings are then compared with a finite difference solution of the Euler Equations for the sonic solution. The usefulness of the shockless, transonic, boundary surfaces appears once transformed to dimensional body

surfaces; "patching" (i.e., translating), the dimensional, subsonic, body surface of $C_p=0$ at the upstream inflow, with the dimensional, sonic body surface, enables us to form complete transonic upper surfaces of interest for design.

II. THE TRANSONIC EQUATION

The small perturbation nonlinear, two dimensional Transonic Equation

$$(1-M_\infty^2) \Phi_{xx} + \Phi_{yy} = \frac{M_\infty^2(\gamma+1)}{U_\infty} \Phi_x \Phi_{xx} \quad (1)$$

is described by the velocity potentials

$$u = \Phi_x \quad v = \Phi_y \quad (2)$$

Multiplying eqn. 1 by $1/U_\infty$ enables us to transform the Transonic Equation to

$$(1-M_\infty^2) \phi_{xx} + \phi_{yy} = M_\infty^2(\gamma+1) \phi_x \phi_{xx} \quad (3)$$

where the nondimensional velocity potentials are

$$\phi_x = \frac{u}{U_\infty} \quad \phi_y = \frac{v}{U_\infty} \quad (4)$$

The Meyer solution for the de-Laval nozzle defines a velocity potential

$$\phi(x, y) = b \left[\frac{x^2}{2} + b(\gamma+1) M_\infty^2 \frac{xy^2}{2} + b^2(\gamma+1)^2 M_\infty^4 \frac{y^4}{24} \right] \quad (5)$$

which satisfies the nondimensional form of equation (3) for $M_\infty=1.0$. The Meyer solution belongs to a general class of sonic flows as reported by Guderley and Yoshihara, [Ref. 4].

The transonic equation (1) may be modified to a more useful form if multiplied by $M_\infty^2(\gamma+1)/U_\infty$, instead of just $1/U_\infty$, to give

$$(1-M_\infty^2)\phi_{xx} + \phi_{yy} = \phi_x\phi_{xx} \quad (6)$$

Here the modified velocity potentials are

$$\phi_x = M_\infty^2(\gamma+1) \frac{u}{U_\infty} \quad \phi_y = M_\infty^2(\gamma+1) \frac{v}{U_\infty} \quad (7)$$

For a given problem, M_∞ and γ are constants, and eqn. 6 is really less cluttered. However, notice that $M_\infty^2(\gamma+1)/U_\infty$ is already given in the derivatives of ϕ in eqns. 7, and therefore appears in the expressions of C_p and the boundary surfaces as will be shown later. This form of the modified transonic equation (6) will be examined in the next chapters.

III. THE GOVERNING DIFFERENTIAL EQUATIONS

An exact solution to the modified transonic equation 6 has been given by Biblarz, [Ref. 2], starting from

$$\phi(x, y) = \phi^s(x, y) + (1 - M_\infty^2) x \quad (8)$$

where $\phi^s(x, y)$ refers to the sonic, small perturbation solution ($M_\infty = 1.0$). In other words, "any flow which satisfies the sonic equation also satisfies the full transonic range with similar boundary conditions," [Ref. 2].

An exact solution may be obtained by using the separation-of-variables approach with the potential function $\phi(x, y)$ of the form

$$\phi(x, y) = \xi(x) \eta(y) + (1 - M_\infty^2) x \quad (9)$$

Substituting the above ϕ function in the modified transonic equation 6 results in two ordinary, second order, nonlinear differential equations

$$\frac{d\xi}{dx} \frac{d^2\xi}{dx^2} - \lambda \xi = 0 \quad (10)$$

$$\frac{d^2\eta}{dy^2} - \lambda \eta^2 = 0 \quad (11)$$

where λ is a separation constant.

A simple solution to the first differential eqn. 10 is obtained by multiplying both sides by $d\xi/dx$,

$$\frac{d\xi}{dx} \left(\frac{d\xi}{dx} \frac{d^2\xi}{dx^2} \right) - \frac{d\xi}{dx} (\lambda \xi) = 0 \quad (12)$$

or

$$\frac{d}{dx} \left[\frac{1}{3} \left(\frac{d\xi}{dx} \right)^3 - \frac{\lambda}{2} \xi^2 \right] = 0 \quad (13)$$

Thus

$$\frac{d\xi}{dx} = \sqrt[3]{\frac{3\lambda}{2} \xi^2 + \alpha} \quad (14)$$

$$dx = \frac{d\xi}{\sqrt[3]{\frac{3\lambda}{2} \xi^2 + \alpha}} \quad (15)$$

and

$$x - x_0 = \int \frac{d\xi}{\sqrt[3]{\frac{3\lambda}{2} \xi^2 + \alpha}} \quad (16)$$

where α and x_0 are integration constants.

A similar procedure can be performed to solve the second differential eqn. 11 yielding

$$\frac{d\eta}{dy} \left(\frac{d^2\eta}{dy^2} \right) - \frac{d\eta}{dy} (\lambda \eta^2) = 0 \quad (17)$$

or

$$\frac{d}{dy} \left[\frac{1}{2} \left(\frac{d\eta}{dy} \right)^2 - \frac{\lambda}{3} \eta^3 \right] = 0 \quad (18)$$

$$\frac{d\eta}{dy} = \pm \sqrt{\frac{2\lambda}{3}\eta^3 + \beta} \quad (19)$$

$$dy = \pm \frac{d\eta}{\sqrt{\frac{2\lambda}{3}\eta^3 + \beta}} \quad (20)$$

and

$$y - y_0 = \pm \int \frac{d\eta}{\sqrt{\frac{2\lambda}{3}\eta^3 + \beta}} \quad (21)$$

where β and y_0 are integration constants.

Egns. 16 and 21 are exact solutions to the differential eqns. 10 and 11. In fact, boundary conditions are needed to evaluate the integration constants α , β , x_0 , y_0 as well as λ . An important step in this procedure is the recognition of α and β as functions of $(1-M_\infty^2)$, [Ref. 2], i.e.,

$$\alpha = \pm C_1 (1-M_\infty^2)^2 \quad (22)$$

$$\beta = \pm C_2 (1-M_\infty^2) \quad (23)$$

The upper positive sign and the lower negative sign in the above equations will be shown to belong to $M_\infty \geq 1.0$ and $M_\infty < 1.0$ respectively, namely,

$$\alpha \geq 0 \text{ \& } \beta \leq 0 \quad \text{for} \quad M_\infty \geq 1.0$$

$$\alpha < 0 \text{ \& } \beta < 0 \quad \text{for} \quad M_\infty < 1.0$$

See Appendix B.

The constants, α , β and λ can be shown to be related by the expression

$$\frac{\alpha\beta}{\lambda} = \frac{2}{3} (1-M_\infty^2)^3 \quad (24)$$

Since C_1 , C_2 and λ are positive constants

$$C_1 C_2 = \frac{2}{3} \lambda \quad (25)$$

The usefulness of these definitions will be outlined in more detail once we use the exact solutions from eqns. 16 and 21, while verifying the correct boundary conditions for the pressure coefficient C_p .

Upon inserting eqns. 22 and 23 in eqns. 16 and 21 we have

$$x - x_0 = \int \frac{d\xi}{\sqrt[3]{\frac{3\lambda}{2} \xi^2 \pm C_1 (1-M_\infty^2)^2}} \quad (26)$$

$$y - y_0 = \pm \int \frac{d\eta}{\sqrt[3]{\frac{2\lambda}{3} \eta^3 \pm C_2 (1-M_\infty^2)}} \quad (27)$$

Factoring out C_1 and C_2 we obtain

$$x - x_0 = C_1^{-\frac{1}{3}} \int \frac{d\xi}{\sqrt[3]{\frac{3\lambda}{2C_1} \xi^2 \pm (1-M_\infty^2)^2}} \quad (28)$$

$$y - y_0 = \pm C_2^{-\frac{1}{2}} \int \frac{d\eta}{\sqrt{\frac{2\lambda}{3C_2} \eta^3 \pm (1-M_\infty^2)}} \quad (29)$$

Introducing new dependent variables

$$\xi \equiv \xi \left(\frac{3\lambda}{2C_1} \right)^{\frac{1}{2}} \quad (30)$$

$$\tilde{\eta} \equiv \eta \left(\frac{2\lambda}{3C_2} \right)^{\frac{1}{3}} \quad (31)$$

the above simply becomes

$$x - x_0 = C_1^{\frac{1}{6}} \left(\frac{3\lambda}{2} \right)^{-\frac{1}{2}} \int \frac{d\xi}{\sqrt{\xi^2 \pm (1-M_\infty^2)^2}} \quad (32)$$

$$y - y_0 = \pm C_2^{-\frac{1}{6}} \left(\frac{2\lambda}{3} \right)^{-\frac{1}{3}} \int \frac{d\tilde{\eta}}{\sqrt{\tilde{\eta}^3 \pm (1-M_\infty^2)}} \quad (33)$$

Finally, if we define new independent variables

$$X \equiv (x - x_0) C_1^{-\frac{1}{6}} \left(\frac{3\lambda}{2} \right)^{\frac{1}{2}} \quad (34)$$

$$Y \equiv (y - y_0) C_2^{\frac{1}{6}} \left(\frac{2\lambda}{3} \right)^{\frac{1}{3}} \quad (35)$$

eqns. 32 and 33 then follow as

$$X = \int \frac{d\xi}{\sqrt[3]{\xi^2 \pm (1-M_\infty^2)^2}} \quad (36)$$

$$Y = \pm \int \frac{d\eta}{\sqrt{\eta^3 \pm (1-M_\infty^2)}} \quad (37)$$

This set will be numerically integrated to obtain transonic surfaces with their corresponding C_p and Mach number profiles.

IV. NUMERICAL INTEGRATION

We can rewrite eqns. 36 and 37 in a more general form and specify the two integral limits

$$X = \int_0^{\pm \xi} \frac{dZ}{\sqrt[3]{Z^2 \pm (1-M_\infty^2)^2}} \quad (38)$$

$$Y = \pm \int_{\mp (1-M_\infty^2)^{\frac{1}{3}}}^{\tilde{\eta}} \frac{dW}{\sqrt{W^3 \pm (1-M_\infty^2)}} \quad (39)$$

As indicated before, the upper and lower sign within the integrand root and the integral limits is used for $M_\infty \geq 1.0$ and $M_\infty < 1.0$ respectively. In addition, our flow of interest is only the first quadrant in X and Y , which represents physical external flows. To show this clearly, for the subsonic case $M_\infty < 1.0$, eqns. 38 and 39 reduce to the form

$$X = \int_0^{\xi} \frac{dZ}{\sqrt[3]{Z^2 - (1-M_\infty^2)^2}} \quad 0 \leq \xi \leq -(1-M_\infty^2)^{\frac{1}{3}} \quad (40)$$

$$Y = - \int_{(1-M_\infty^2)^{\frac{1}{3}}}^{\tilde{\eta}} \frac{dW}{\sqrt{W^3 - (1-M_\infty^2)}} \quad \tilde{\eta} \geq (1-M_\infty^2)^{\frac{1}{3}} \quad (41)$$

and for $M_\infty \geq 1.0$ we have

$$X = \int_0^{\xi} \frac{dZ}{\sqrt[3]{Z^2 + (1-M_\infty^2)^2}} \quad \xi \geq 0 \quad (42)$$

$$Y = - \int_{-(1-M_\infty^2)^{\frac{1}{3}}}^{\bar{\eta}} \frac{dW}{\sqrt{W^3 + (1-M_\infty^2)}} \quad \bar{\eta} \geq -(1-M_\infty^2)^{\frac{1}{3}} \quad (43)$$

However, we will frequently retain the more general " \pm " notation in our discussions further on.

Before we head to numerical solutions, we should indicate that sonic flow ($M_\infty=1.0$) can be given in explicit form through eqns. 40,41,42,43, i.e., the resulting equations for sonic flow are

$$X = \int_0^{\xi} \frac{dZ}{\sqrt[3]{Z^2}} \quad (44)$$

$$Y = - \int_0^{\bar{\eta}} \frac{dW}{\sqrt{W^3}} \quad (45)$$

Solving equations 44 and 45 we obtain our sonic solution

$$\xi = \left(\frac{1}{3} X \right)^3 \quad (46)$$

$$\bar{\eta} = \left(\frac{2}{Y} \right)^2 \quad (47)$$

Having defined $\tilde{\xi}, \tilde{\eta}, X$ and Y in eqns. 30,31 and eqns. 34,35, we can express the sonic solution rewriting eqns. 46 and 47 as

$$\xi = \frac{1}{3^3} (x-x_0)^3 \left(\frac{3\lambda}{2} \right) \quad (48)$$

$$\eta = \frac{2^2}{(y-y_0)^2 \left(\frac{2\lambda}{3} \right)} \quad (49)$$

Providing the sonic perturbation potential from eqn. 9

$$\phi^s = \xi \eta \quad (50)$$

and inserting eqns. 48 and 49 we have, [Ref. 2]

$$\phi^s = \frac{1}{3} \frac{(x-x_0)^3}{(y-y_0)^2} \quad (51)$$

Next, eqns. 40 to 43 are numerically integrated and plotted in Figs. 1 and 2 for various M_∞ , (e.g., 0.8, 0.9, 1.0, 1.1, 1.2). Plotting $\tilde{\eta}$ vs. Y for $Y > 0$ in Fig. 2 is an appropriate choice for investigating physical external flows as stated earlier.

Our numerical solution has been based upon the Newton-Cotes method of order 4, [Ref. 5], which may be applied to an even number of subintervals, each described as,

$$\int_a^b f(x) dx = \frac{(b-a)}{90} \left[7 f(a) + 32 f\left(\frac{a+b}{4}\right) + 12 f\left(\frac{a+b}{2}\right) + 32 f\left(\frac{3(a+b)}{4}\right) + 7 f(b) \right] \quad (52)$$

(See appendix A).

Numerical solutions which express $\tilde{\xi}$ and $\tilde{\eta}$, as has been noted, can be combined with eqns. 30,31 and eqns. 34,35 and substituted in eqn. 9 to give a complete solution for the perturbation potential in terms of the positive constants λ or (C_1, C_2) , and (x_0, y_0) .

V. BOUNDARY SURFACES

For an inviscid flow, the condition to be applied at the surface of a solid boundary is that the direction of the flow velocity vector is tangent to the solid surface, [Ref. 6]. In terms of perturbation velocities this boundary condition becomes

$$\left(\frac{dy}{dx}\right)_{\text{surface}} = \frac{v}{U_\infty} \quad (53)$$

The modified velocity perturbation potential as pointed out earlier is

$$\phi_y = M_\infty^2 (\gamma + 1) \frac{v}{U_\infty} \quad (54)$$

thus

$$\frac{v}{U_\infty} = \frac{\phi_y}{M_\infty^2 (\gamma + 1)} \quad (55)$$

We can show by substitution that

$$\left(\frac{dy}{dx}\right)_{\text{surface}} = \frac{\phi_y}{M_\infty^2 (\gamma + 1)} \quad (56)$$

Now, deriving the perturbed potential function in eqn. 9 with respect to y gives

$$\phi_y = \xi \frac{d\eta}{dy} \quad (57)$$

Eqn. 19 for $y > 0$ becomes

$$\frac{d\eta}{dy} = -\sqrt{\frac{2\lambda}{3}\eta^3 + \beta} \quad (58)$$

This relation can be rearranged using $\tilde{\eta}$ and β in eqns. 31 and 23 to yield

$$\frac{d\eta}{dy} = -C_2^{\frac{1}{2}} \sqrt{\tilde{\eta}^3 \pm (1-M_\infty^2)} \quad (59)$$

Upon using this equation and the relation of eqn. 30 to the derived velocity potential in eqn. 57 results in

$$\phi_y = -\xi \left(\frac{3\lambda}{2C_1} \right)^{-\frac{1}{2}} C_2^{\frac{1}{2}} \sqrt{\tilde{\eta}^3 \pm (1-M_\infty^2)} \quad (60)$$

The last equation can be rewritten with the benefit of the related constants C_1 , C_2 and λ in eqn. 25, hence

$$\phi_y = -\frac{2}{3} \xi \sqrt{\tilde{\eta}^3 \pm (1-M_\infty^2)} \quad (61)$$

Once we have found the form of ϕ_y , the expression for the surface boundary condition is given as

$$\left(\frac{dy}{dx} \right)_{\text{surface}} = -\frac{2}{3} \frac{1}{M_\infty^2(\gamma+1)} \xi \sqrt{\tilde{\eta}^3 \pm (1-M_\infty^2)} \quad (62)$$

However, an important result to observe is that $\tilde{\xi}$ and $\tilde{\eta}$ in the R.H.S. of this equation are given implicitly as a function of x and y respectively in our earlier numerical integration solution, while the L.H.S. is expressed by x and y . To get

compatibility, we then transform the L.H.S. of eqn. 62 using the chain rule

$$\frac{dy}{dx} = \frac{dY}{dX} \frac{dX/dx}{dY/dy} \quad (63)$$

Deriving eqn. 34 with respect to x and eqn. 35 with respect to y gives

$$\frac{dX}{dx} = C_1^{-\frac{1}{6}} \left(\frac{3\lambda}{2} \right)^{\frac{1}{2}} \quad (64)$$

$$\frac{dY}{dy} = C_2^{\frac{1}{6}} \left(\frac{2\lambda}{3} \right)^{\frac{1}{3}} \quad (65)$$

therefore

$$\frac{dy}{dx} = \frac{3}{2} \frac{dY}{dX} \quad (66)$$

Equation 62 can be rewritten using the above transformation as

$$\frac{dY}{dX} = -\left(\frac{2}{3}\right)^2 \frac{1}{M_\infty^2 (\gamma+1)} \xi \sqrt{\tilde{\eta}^3 \pm (1-M_\infty^2)} \quad (67)$$

or

$$\frac{dY}{\sqrt{\tilde{\eta}^3 \pm (1-M_\infty^2)}} = -\left(\frac{2}{3}\right)^2 \frac{1}{M_\infty^2 (\gamma+1)} \xi dX \quad (68)$$

We are now in a position to compute the exact boundary surfaces out of eqn. 68. Starting with the L.H.S. we then define

$$E(Y) = \frac{1}{\sqrt{\tilde{\eta}^3 \pm (1-M_\infty^2)}} \quad (69)$$

Having defined eqn. 69 we can plot $E(Y)$ vs. Y in Fig. 3 for various M_∞ , (e.g., 0.8, 0.9, 1.0, 1.1, 1.2), keeping in mind our " \pm " notation for the supersonic (upper sign) and subsonic (lower sign).

The asymptotic value of $E(Y)$ occurs at Y_0 where

$$\tilde{\eta} \rightarrow \mp (1 - M_\infty^2)^{\frac{1}{3}} \quad (70)$$

In other words, the asymptotic value can be expressed as $Y_0 = Y_0(M_\infty)$, or as function of $(1 - M_\infty^2)$, which has been numerically found to be

$$Y_0 \approx \frac{2.4}{|1 - M_\infty^2|^{\frac{1}{6}}} \quad (71)$$

Y_0 vs. M_∞ is sketched in Fig. 4 to demonstrate an interesting symmetry with respect to $M_\infty = 1.0$. Here $Y_0 = \infty$ but note that for practical reasons we can adopt finite values of Y_0 (perhaps as low as 7 to 20) to represent conditions sufficiently close to $M_\infty = 1.0$.

Defining the integral of the R.H.S. of eqn. 68 as

$$K(X) = -\left(\frac{2}{3}\right)^2 \frac{1}{M_\infty^2 (\gamma + 1)} \int_0^X \xi \, d\tilde{X} \quad (72)$$

and redoing numerical integration allow us to plot $K(X)$ vs. X for $\gamma = 1.4$ in Fig. 5. It is important to realize that $K(X) > 0$ for $M_\infty < 1.0$ and $K(X) < 0$ for $M_\infty \geq 1.0$, before solving eqn. 68.

Therefore, integrating both sides of eqn. 68 yields for $K(X) > 0$

$$\int_Y^{Y_0} E(\tilde{Y}) d\tilde{Y} = K(X) \quad (73)$$

and for $K(X) < 0$

$$\int_{Y_0}^Y E(\tilde{Y}) d\tilde{Y} = K(X) \quad (74)$$

Once we specify X for $K(X)$ we can immediately solve the L.H.S. integrals of eqns. 73 and 74 for Y , expressing

$$(Y)_{\text{surface}} = Y(X) \quad (75)$$

namely, the required boundary surface for any chosen M_∞ .

We can rewrite eqns. 73 and 74 in the more complete form for $M_\infty < 1.0$ as

$$\int_Y^{Y_0} \frac{d\tilde{Y}}{\sqrt{\tilde{\eta}^3 - (1-M_\infty^2)}} = -\left(\frac{2}{3}\right)^2 \frac{1}{M_\infty^2(\gamma+1)} \int_0^X \xi d\tilde{X} \quad (76)$$

and for $M_\infty \geq 1.0$

$$\int_{Y_0}^Y \frac{d\tilde{Y}}{\sqrt{\tilde{\eta}^3 + (1-M_\infty^2)}} = -\left(\frac{2}{3}\right)^2 \frac{1}{M_\infty^2(\gamma+1)} \int_0^X \xi d\tilde{X} \quad (77)$$

Eqns. 76 and 77 are equivalent to eqns. 73 and 74 which finally yield the boundary surfaces. These are shown nondimensionally in Figs. 6 and 7 for $M_\infty = 0.8, 0.9, 0.97$ and in Fig. 8 for $M_\infty = 1.0, 1.1, 1.2$.

The sonic surface is most easily verified by direct analytical expansion of eqn. 77, using the sonic relations stated in eqns. 46 and 47.

$$\int_{Y_0}^Y \left(\frac{2}{\tilde{Y}} \right)^{-3} d\tilde{Y} = - \left(\frac{2}{3} \right)^2 \frac{1}{(\gamma+1)} \int_0^X \left(\frac{1}{3} \tilde{X} \right)^3 d\tilde{X} \quad (78)$$

Solving the above integrals on both sides gives

$$Y^4 - Y_0^4 = - \frac{1}{(\gamma+1)} \left(\frac{2}{3} \right)^5 X^4 \quad (79)$$

Recall that $Y_0 \rightarrow \infty$ for the sonic case. However, choosing for example $Y_0=20$ gives an asymptotic value of $\tilde{\eta}=0.01$, (eqn. 47), and $E(Y_0)=1000$, (eqn. 69), for our explicit sonic solution. (See also Figs. 2 and 3). Therefore, dividing by a finite Y_0 enables us to obtain the nondimensional sonic boundary surface as a function of γ .

$$\frac{Y}{Y_0} = \sqrt[4]{1 - \frac{1}{(\gamma+1)} \left(\frac{2}{3} \right)^5 \left(\frac{X}{Y_0} \right)^4} \quad (80)$$

This will be shown to be a divergent surface which increases the Mach number to supersonic conditions.

VI. PRESSURE COEFFICIENT

For a flow with small perturbations the pressure coefficient is given by, [Ref. 8]

$$C_p = - \left[\frac{2u}{U_\infty} + (1-M_\infty^2) \left(\frac{u}{U_\infty} \right)^2 + \left(\frac{v}{U_\infty} \right)^2 \right] \quad (81)$$

A first order approximation for the linearized pressure coefficient in a two dimensional planar flow is

$$C_p = - \frac{2u}{U_\infty} \quad (82)$$

Recall the modified velocity potential

$$\phi_x = M_\infty^2 (\gamma+1) \frac{u}{U_\infty} \quad (83)$$

Thus

$$\frac{u}{U_\infty} = \frac{\phi_x}{M_\infty^2 (\gamma+1)} \quad (84)$$

and from eqn. 82 we see that

$$C_p = - \frac{2\phi_x}{M_\infty^2 (\gamma+1)} \quad (85)$$

Now, deriving the potential function in eqn. 9 with respect to x we have

$$\phi_x = \frac{d\xi}{dx} + (1-M_\infty^2) \quad (86)$$

Rewriting eqn. 14 using the relation for α in eqn. 22 as

$$\frac{d\xi}{dx} = \sqrt[3]{\frac{3\lambda}{2}\xi^2 \pm C_1(1-M_\infty^2)^2} \quad (87)$$

By taking advantage of $\tilde{\xi}$ as stated in eqn. 31 and factoring out C_1 , eqn. 87 becomes

$$\frac{d\xi}{dx} = C_1^{\frac{1}{3}} \sqrt[3]{\xi^2 \pm (1-M_\infty^2)^2} \quad (88)$$

Substituting eqn. 88 and the relation for $\tilde{\eta}$ in eqn. 31 to the velocity potential ϕ_x in eqn. 86 yields

$$\phi_x = \tilde{\eta} \left(\frac{3C_1C_2}{2\lambda} \right)^{\frac{1}{3}} \sqrt[3]{\xi^2 \pm (1-M_\infty^2)^2} + (1-M_\infty^2) \quad (89)$$

Once again, using the benefit of the related constants C_1 , C_2 and λ in eqn. 25, eqn. 89 becomes

$$\phi_x = \tilde{\eta} \sqrt[3]{\xi^2 \pm (1-M_\infty^2)^2} + (1-M_\infty^2) \quad (90)$$

therefore eqn. 85 for C_p follows as

$$C_p = \frac{-2}{M_\infty^2(\gamma+1)} \left[\tilde{\eta} \sqrt[3]{\xi^2 \pm (1-M_\infty^2)^2} + (1-M_\infty^2) \right] \quad (91)$$

We must anticipate the above expression for C_p to satisfy the boundary conditions on external boundary surfaces as will be explored further on.

VII. THE LOCAL MACH NUMBER

The velocity vector \vec{V} is given by the undisturbed uniform velocity U_∞ and the perturbation velocities for the 2D flow as

$$\vec{V} = \vec{i}(U_\infty + u) + \vec{j}v \quad (92)$$

Thus, we may obtain the local Mach number M in terms of the above velocities and the local speed of sound "a".

$$M^2 = \frac{|\vec{V}|^2}{a^2} = \frac{(U_\infty + u)^2 + v^2}{a^2} \quad (93)$$

Neglecting higher powers of the perturbation velocities gives

$$M^2 = \frac{U_\infty^2 \left(1 + \frac{2u}{U_\infty}\right)}{a^2} \quad (94)$$

In addition, the ratio of the local speed of sound to the undisturbed uniform speed of sound becomes

$$\frac{a^2}{a_\infty^2} = \frac{T}{T_\infty} \quad (95)$$

or

$$\frac{a^2}{a_\infty^2} = \frac{T_0/T_\infty}{T_0/T} \quad (96)$$

where T_0 designates the stagnation temperature.

Eqn. 96 can be replaced using the well known relation

$$\frac{a^2}{a_\infty^2} = \frac{1 + \frac{\gamma-1}{2} M_\infty^2}{1 + \frac{\gamma-1}{2} M^2} \quad (97)$$

Substituting the local speed of sound from eqn. 97 to eqn. 94 results as

$$M^2 = M_\infty^2 \frac{\left(1 + \frac{2u}{U_\infty}\right)}{\left(\frac{1 + \frac{\gamma-1}{2} M_\infty^2}{1 + \frac{\gamma-1}{2} M^2}\right)} \quad (98)$$

Having stated C_p in eqn. 82, eqn. 98 is reduced to the form

$$\frac{M^2}{1 + \frac{\gamma-1}{2} M^2} = \frac{M_\infty^2 (1 - C_p)}{1 + \frac{\gamma-1}{2} M_\infty^2} \quad (99)$$

Rearranging eqn. 99 and factoring out M^2 yields the final expression for the local Mach number

$$M^2 = \frac{M_\infty^2 (1 - C_p)}{1 + \frac{\gamma-1}{2} M_\infty^2 C_p} \quad (100)$$

Note that $M=M_\infty$ when $C_p=0$ as it should.

This important relation, combined with the corresponding eqn. 91 for C_p , will be used when discussing the boundary conditions in the next chapter.

VIII. BOUNDARY CONDITIONS

Rather than providing the boundary conditions for the governing differential eqns. 10 and 11 to evaluate the constants, we imposed a solution by defining α and β in eqns. 22 and 23 respectively. That is to say, boundary conditions have been already implied in the definitions of α and β . This procedure led us to reveal the boundary surfaces upon using the tangency condition and compute the pressure coefficient C_p on the body surface, (eqn. 91).

Thus, we arrive at the necessity to verify the validity of the expression for C_p for the boundary surface, and verify the following requirements:

- At the upstream end ($X/Y_0=0$), we must require that $C_p=0$ ensuring the unperturbed Mach number of the transonic inflow to equal M_∞ .
- For the subsonic inflow at the downstream end ($X @ Y/Y_0=1$) we must require that the local Mach number saturates towards $M=1.0$. This is because of the well known relation in gas dynamics for a convergent flow.

We first restrict our attention to the first requirement, for $M_\infty \geq 1.0$ at $X/Y_0=0$

$$\xi = \xi^* = 0 \quad (101)$$

At $Y/Y_0=1$ eqn. 70 becomes

$$\tilde{\eta} - \tilde{\eta}^* = -(1 - M_\infty^2)^{\frac{1}{3}} \quad (102)$$

Inserting the above terms of $\tilde{\xi}$ and $\tilde{\eta}$ in eqns. 90 and 91 gives

$$\phi_x = -(1-M_\infty^2)^{\frac{1}{3}} \sqrt[3]{(1-M_\infty^2)^2} + (1-M_\infty^2) = 0 \quad (103)$$

and

$$C_p @ (X/Y_0 = 0, Y/Y_0 = 1) = 0 \quad (104)$$

Therefore, from eqn. 100

$$M @ (X/Y_0 = 0, Y/Y_0 = 1) = M_\infty \quad (105)$$

Hence, eqns. 104 and 105 comply with the first requirement. The complete behavior of the pressure coefficient and the local Mach number are plotted in Figs. 9 and 10 for $M_\infty=1.0$ and $M_\infty=1.1$. In addition, it is important to note that the boundary surfaces ought to be truncated at $M_\infty \leq 1.2$, so as not to exceed the small perturbation assumptions.

Now, for $M_\infty < 1.0$ at $X/Y_0=0$

$$\xi = \xi^* = 0 \quad (106)$$

However, at $Y/Y_0=0$

$$\tilde{\eta} \rightarrow \tilde{\eta}^* = \infty \quad (107)$$

Thus, eqn. 91 results as

$$C_p @ (X/Y_0 = 0, Y/Y_0 = 0) \rightarrow \infty \quad (108)$$

We immediately conclude that the above coordinate (0,0) can not serve as the upstream start for the subsonic inflow. Instead, we must localize a new upstream end coordinate along the boundary surface whose $\tilde{\xi}^*$ and $\tilde{\eta}^*$ values satisfy eqn. 91

for the equality $C_p=0$. Since every coordinate on the boundary surface $(X/Y_0, Y/Y_0)$ is a function of $\tilde{\xi}$ and $\tilde{\eta}$, (eqn. 76), we can numerically scan the locus of all the coordinates, i.e., the boundary surface, for such values of $\tilde{\xi}^*$ and $\tilde{\eta}^*$ that will satisfy eqn. 91. For example, scanning the results for the subsonic boundary surface of $M_\infty=0.8$ reveals; $\tilde{\xi}=\tilde{\xi}^*=-0.35763$ and $\tilde{\eta}=\tilde{\eta}^*=3.01393$ at the coordinate $(X/Y_0=0.31366, Y/Y_0=0.40616)$. Inserting the above values of $\tilde{\xi}^*$ and $\tilde{\eta}^*$ in eqn. 91 yields $C_p=0.0003$. Hence, by relocating a new upstream coordinate for the subsonic inflow we are then able to satisfy our first requirement. (This is shown later in Figs. 11 and 12).

We now consider the second requirement for the subsonic outflow at the downstream end where

$$\tilde{\xi} - \tilde{\xi}^* = -(1 - M_\infty^2) \quad (109)$$

$$\tilde{\eta} @ (Y/Y_0=1) - \tilde{\eta}^* = (1 - M_\infty^2)^{\frac{1}{3}} \quad (110)$$

or equivalently $dY/dX \rightarrow 0$

Substituting these terms for $\tilde{\xi}$ and $\tilde{\eta}$ in eqns. 90 and 91 gives

$$\phi_x = (1 - M_\infty^2) \quad (111)$$

and

$$C_p = \frac{-2(1 - M_\infty^2)}{M_\infty^2(\gamma + 1)} \quad (112)$$

Thus, we can express the local Mach number using eqn. 100

$$M^2 = \frac{M_\infty^2 \left(1 + \frac{2(1-M_\infty^2)}{M_\infty^2(\gamma+1)} \right)}{1 - \frac{(\gamma-1)}{2} M_\infty^2 \frac{2(1-M_\infty^2)}{M_\infty^2(\gamma+1)}} \quad (113)$$

Upon expanding eqn. 113 and factoring out M_∞^2 we obtain

$$M^2 = \frac{M_\infty^2(\gamma-1) + 2}{M_\infty^2(\gamma-1) + 2} \quad (114)$$

or equivalently

$$M = 1 \quad (115)$$

Hence, we have verified the second requirement: The local Mach number saturates at the downstream end to the value $M=1.0$ for any subsonic inflow $M_\infty < 1.0$. The pressure coefficient and the local Mach number behavior along the boundary surface are plotted in Figs. 11 and 12 for $M_\infty=0.8$ and $M_\infty=0.9$ respectively, showing clearly both the upstream and downstream boundary conditions.

Knowing that boundary conditions require the gradient of the potential function ϕ to vanish far away from the body gives rise to an important question: How is the flow pattern along the boundary surface propagated into the flow field? We treat this question by considering a computationally efficient flow solver developed by J. A. Ekaterinaris, [Ref. 7]. This CFD solver consists of the inviscid Euler equations and uses fully implicit two dimensional Crank-Nicholson method with a

central difference ADI scheme, and fourth and second order numerical dissipation, [Ref. 9]. This solver has been modified here to solve the inviscid flow around our earlier boundary surface solution for the chosen sonic case $M_\infty=1.0$. By creating a grid mesh which consists of a boundary surface edge, we are able to map the flow pattern. Upon observing the constant Mach lines as graphed in Fig. 14, we deduce that the flow is shockless through the whole transonic range; a shock is formed further downstream at the local Mach number $M=1.9$. These results are in complete accordance with the inviscid small perturbation transonic solution, (see Fig. 9). In addition, each vector on Fig. 13 describes the resultant flow direction at a specified grid point, (not the streamlines !), colored by Mach levels. Thereby, we may evidence the far-field boundary conditions

$$\mathbf{V} = U_\infty \quad u = v = 0 \quad (116)$$

In other words, the flow pattern is propagated out from the boundary surface gradually towards satisfying the far-field boundary conditions far away from the body.

It is of special interest to inspect the dimensional boundary surface for possible design applications; For example, the dimensional, subsonic, boundary surface of $M_\infty=0.8$ is obtained by multiplying the nondimensional coordinates $(X/Y_{0(0.8)}, Y/Y_{0(0.8)})$ by $Y_{0(0.8)}=2.84$, i.e., the dimensional, downstream end coordinate results as $(X_1, 2.84)$,

as plotted in Fig. 15a. Similarly, multiplying the nondimensional, sonic coordinates $(X/Y_{0(1.0)}, Y/Y_{0(1.0)})$ by $Y_{0(1.0)}=14$, yields the dimensional, sonic, boundary surface, where the dimensional, upstream, starting coordinate becomes $(0,14)$. Now, translating the dimensional, sonic, boundary surface, (Fig. 15b), by $(\Delta X, \Delta Y) = (X_1, -(14-2.84))$, to match the downstream end coordinate of the above dimensional, subsonic, boundary surface, "patches" both dimensional boundary surfaces, to form a 2D planar upper surface as shown in Fig. 15. We may use this technique to "patch" any subsonic boundary surface in order to form our transonic upper surface of interest.

IX. CONCLUSIONS

We have shown that an exact solution for the transonic equation satisfies the complete behavior of the pressure coefficient, and the local Mach along a 2D-surface for planar, external flow. It is of special interest to inspect the dimensional boundary surface for possible design applications; For example, the dimensional, subsonic, and sonic boundary surfaces are obtained by multiplying the nondimensional coordinates $(X/Y_0, Y/Y_0)$, by the corresponding Y_0 . Translation of the dimensional, sonic, boundary surface, to match the downstream end coordinate of the above dimensional, subsonic, boundary surface, "patches" both dimensional boundary surfaces, to form a 2D planar upper surface as shown in Fig. 15. This technique may serve as a powerful tool for the implementation of supercritical, shockless, planar surface designs, because of the saturation of $\tilde{\eta}$ with Y (Fig. 2), we can also describe certain internal flows such as planar converging, diverging tunnel walls. We may also extend these results to axisymmetric transonic flow.

LIST OF REFERENCES

1. Nixon, D., "Transonic Aerodynamics," AIAA, Progress in Astronautics and Aeronautics, Vol. 81, 1982.
2. Biblarz, O., "Phase Plane Analysis of Transonic Flows," AIAA, Paper No. 76-332, July 1976.
3. Biblarz, O., "An Exact Solution to the Transonic Equation," Israel Journal of Technology, Vol. 13, pg. 229. 1975.
4. Guderley, K. G., "The theory of Transonic Flow," Pergamon Press, London 1962.
5. Arden, W. B., Astill, N. K., "Numerical Algorithms: Origins and Applications," Addison-Wesley Publishing Company, Inc. 1970.
6. Zucrow, M. J., Hoffman, J. D., "Gas Dynamics," Vol. I & II, John Wiley and Sons, Inc. 1976.
7. Clarkson, J. D., Ekaterinaris, J. A., and Platzer, M. F., "Computational Investigation of Airfoil Stall Flutter," 6th International Symposium on Unsteady Aerodynamics, Aeroacoustics and Aeroelasticity, Sept. 1991.
8. Liepmann, H. W., Roshko, A., "Elements of Gas Dynamics," John Wiley and Sons, Inc. 1957.
9. Anderson, A. D., Tannehill, C. J., and Pletcher, H. R., "Computational Fluid Mechanics and Heat Transfer," Hemisphere Publishing Corporation, 1984.

APPENDIX A COMPUTER PROGRAMS

```

C*****
*   THIS FORTRAN PROGRAM USES NUMERICAL INTEGRATION BASED ON
THE NEWTON-COTES FORMULA TO SOLVE NUMERICALLY EQNS. 40 AND 42.

```

THE OUTPUT IS IN THE FORM OF $\tilde{\xi}$ vs. X

```

*****

```

```

program KSI
PARAMETER (N=5)
IMPLICIT REAL*8 (A-H,O-Z)
IMPLICIT REAL*8 (M)
IMPLICIT REAL*8 (K)
INTEGER INDEX, I
DIMENSION X (N), XDOT (N), SAVEX (N), SAVED (N), KSI (N)
DIMENSION MACH (N), X1 (N), X2 (N)

```

```

MACH (1)=0.8D0
MACH (2)=0.9D0
MACH (3)=1.0D0
MACH (4)=1.1D0
MACH (5)=1.2D0

```

```

KSI (1)=0.0D0
KSI (2)=0.0D0
KSI (3)=1.0D-3
KSI (4)=0.0D0
KSI (5)=0.0D0

```

```

C*****

```

```

C                               MAIN PROGRAM                               *

```

```

C*****

```

```

DO 100 I=1,5
  IF (I.LT.3) THEN
    H=-0.001D0
    GOTO 5
  END IF
  H=0.01D0
5  IF (I.LT.3) THEN
    TF=- (1.0D0-MACH (I)**2)
    GOTO 10
  END IF
  TF=120.0D0
10 IF (I.LT.3.AND.KSI (I).GT.TF.OR.
    I.GE.3.AND.KSI (I).LE.TF) THEN
30  do 50 index=1,5
    CALL DERIVative (KSI,N,I,X1,X2,XDOT,MACH)
    CALL NEWTONCOTES (KSI,XDOT,X,SAVEX,SAVED,H,N,INDEX,I)
50  end do

```

```

        WRITE(10+i,*) X(I),KSI(I)
        GOTO 10
    END IF
100 END DO
    STOP
    END
C*****
C          SUBROUTINE DERIVative
C*****
    SUBROUTINE DERIVative(KSI,N,I,X1,X2,XDOT,MACH)
    IMPLICIT REAL*8(A-H,O-Z)
    IMPLICIT REAL*8(M)
    IMPLICIT REAL*8(K)
    DIMENSION XDOT(N),X1(N),X2(N),KSI(N),MACH(N)
    GO TO (20,20,10,10,10),I
10  X1(I)=KSI(I)**2+(1.0D0-MACH(I)**2)**2
    X2(I)=X1(I)**(1.0D0/3.0D0)
    XDOT(I)=1.0D0/X2(I)
    GOTO 30

20  X1(I)=- (KSI(I)**2-(1.0D0-MACH(I)**2)**2)
    X2(I)=-X1(I)**(1.0D0/3.0D0)
    XDOT(I)=1.0D0/X2(I)
30  RETURN
    END
C*****
C          SUBROUTINE NEWTONCOTES
C*****
    SUBROUTINE NEWTONCOTES(KSI,XDOT,X,SAVEX,SAVED,H,N,INDEX,I)
    IMPLICIT REAL*8(A-H,O-Z)
    IMPLICIT REAL*8(M)
    IMPLICIT REAL*8(K)
    DIMENSION X(N),XDOT(N),SAVEX(N),SAVED(N),KSI(N)
    GO TO (1,2,3,4,5),index
1  SAVEX(I)=X(I)
    SAVED(I)=XDOT(I)
    KSI(I)=KSI(I)+0.25D0*H
    RETURN
2  SAVED(I)=7.0D0*SAVED(I)+32.0D0*XDOT(I)
    KSI(I)=KSI(I)+0.25D0*H
    RETURN
3  SAVED(I)=SAVED(I)+12.0D0*XDOT(I)
    KSI(I)=KSI(I)+0.25D0*H
    RETURN
4  SAVED(I)=SAVED(I)+32.0D0*XDOT(I)
    KSI(I)=KSI(I)+0.25D0*H
    RETURN
5  X(I)=SAVEX(I)+(H/90.0D0)*(SAVED(I)+7.0D0*XDOT(I))
    RETURN
    END
C*****

```

 THIS FORTRAN PROGRAM USES NUMERICAL INTEGRATION BASED ON
 THE NEWTON-COTES FORMULA TO SOLVE NUMERICALLY EQNS. 41 AND 43.

THE OUTPUT IS IN THE FORM OF $\tilde{\eta}$ vs. Y

```

program ETTA
  PARAMETER (N=5)
  PARAMETER (K=2000)
  IMPLICIT REAL*8(A-H,O-Z)
  IMPLICIT REAL*8(M)
  INTEGER INDEX,I,J
  DIMENSION Y(N),YDOT(N),SAVEY(N),SAVED(N),TF(N),MACH(N)
  DIMENSION ETA(N),ETA11(K),Y11(K),Y1(N),Y2(N)
  MACH(1)=0.8D0
  MACH(2)=0.9D0
  MACH(3)=1.0D0
  MACH(4)=1.1D0
  MACH(5)=1.2D0
  H=0.01D0
C*****
C          INTEGRAL FINAL LIMITS          *
C*****
  DO 7 I=1,5
    IF(MACH(I).EQ.1.0D0) THEN
      TF(I)=0.0D0
      GOTO 7
    END IF
    IF(MACH(I).GT.1.0D0) THEN
      TF(I)=(- (1.0D0-MACH(I)**2))** (1.0D0/3.0D0)
      GOTO 7
    END IF
    TF(I)=(1.0D0-MACH(I)**2)** (1.0D0/3.0D0)
7  END DO
C*****
C          MAIN PROGRAM          *
C*****
  DO 100 I=1,5
    J=1
    ETA(I)=14.0D0
    Y(I)=2.0D0/(ETA(I)** (1.0D0/2.0D0))
10  IF(ETA(I)-H.GT.TF(I)) THEN
20    do 50 index=1,5
      CALL DERIVative(ETA,N,I,Y1,Y2,YDOT,MACH)
      CALL NEWTONCOTES(ETA,YDOT,Y,SAVEY,SAVED,H,N,INDEX,I)
50    end do
    ETA11(J)=ETA(I)
    Y11(J)=Y(I)
    J=J+1
    GOTO 10
  END IF
  
```

```

      H=0.001D0
      IF(ETA(I)-H.GT.TF(I)) THEN
        GOTO 20
      END IF
80    DO 90 L=J-1,1,-1
        WRITE(20+i,*) Y11(L),ETA11(L)
90    END DO
100  END DO
      STOP
      END
C*****
C          SUBROUTINE DERIVative
C*****
      SUBROUTINE DERIVative(ETA,N,I,Y1,Y2,YDOT,MACH)
      IMPLICIT REAL*8(A-H,O-Z)
      IMPLICIT REAL*8(M)
      DIMENSION YDOT(N),Y1(N),Y2(N),ETA(N),MACH(N)
      GO TO (20,20,10,10,10),I
10    Y1(I)=ETA(I)**3+(1.0D0-MACH(I)**2)
      Y2(I)=Y1(I)**(1.0D0/2.0D0)
      YDOT(I)=1.0D0/Y2(I)
      GOTO 30
20    Y1(I)=ETA(I)**3-(1.0D0-MACH(I)**2)
      Y2(I)=Y1(I)**(1.0D0/2.0D0)
      YDOT(I)=1.0D0/Y2(I)
30    RETURN
      END
C*****
C          SUBROUTINE NEWTONCOTES
C*****
      SUBROUTINE NEWTONCOTES(ETA,YDOT,Y,SAVEY,SAVED,H,N,INDEX,I)
      IMPLICIT REAL*8(A-H,O-Z)
      IMPLICIT REAL*8(M)
      DIMENSION Y(N),YDOT(N),SAVEY(N),SAVED(N),ETA(N)
      GO TO (1,2,3,4,5),index
1    SAVEY(I)=Y(I)
      SAVED(I)=YDOT(I)
      ETA(I)=ETA(I)-0.25D0*H
      RETURN
2    SAVED(I)=7.0D0*SAVED(I)+32.0D0*YDOT(I)
      ETA(I)=ETA(I)-0.25D0*H
      RETURN
3    SAVED(I)=SAVED(I)+12.0D0*YDOT(I)
      ETA(I)=ETA(I)-0.25D0*H
      RETURN
4    SAVED(I)=SAVED(I)+32.0D0*YDOT(I)
      ETA(I)=ETA(I)-0.25D0*H
      RETURN
5    Y(I)=SAVEY(I)+(H/90.0D0)*(SAVED(I)+7.0D0*YDOT(I))
      RETURN
      END

```

APPENDIX B
FORM OF α AND β

The expressions for α and β as introduced in [REF. 2] are

$$\alpha = \pm C_1 (1 - M_\infty^2)^2 \quad (117)$$

$$\beta = +C_2 (1 - M_\infty^2) \quad (118)$$

for $0.8 \leq M_\infty \leq 1.2$.

Upon inserting eqns. 117 and 118 in eqns. 16 and 21 yields

$$X = \int_0^{\xi} \frac{dZ}{\sqrt[3]{Z^2 + (1 - M_\infty^2)^2}} \quad (119)$$

$$Y = - \int_{-(1 - M_\infty^2)^{\frac{1}{3}}}^{\eta} \frac{dW}{\sqrt{W^3 + (1 - M_\infty^2)}} \quad (120)$$

These relations are numerically integrated and plotted in Figs. 16 and 17. We observe the same solutions for $M_\infty \geq 1.0$ as expected, but distinguish a different set of solutions for the subsonic case $M_\infty < 1.0$.

Applying the same procedure as in Chap. IV, we easily compute the expression for the boundary surfaces

$$\frac{dY}{\sqrt{\eta^3 + (1 - M_\infty^2)}} = - \left(\frac{2}{3}\right)^2 \frac{1}{M_\infty^2 (\gamma + 1)} \xi dX \quad (121)$$

The numerical integration of eqn. 121 is shown in Fig. 18 for various M_∞ , (e.g., 0.8, 0.9, 0.97, 1.0, 1.1, 1.2). The diverging contours of the subsonic solutions appear to give contradictory results once investigating the pressure coefficient behavior

$$C_p = \frac{-2}{M_\infty^2(\gamma+1)} \left[\tilde{\eta} \sqrt[3]{\xi^2 + (1-M_\infty^2)^2} + (1-M_\infty^2) \right] \quad (122)$$

along the boundary surface. This implies as shown in Fig. 19 that the boundary surface within the portion of $C_p > 1.0$ is not a realistic solution.

APPENDIX C
FIGURES

KSI(X) for $M_\infty=0.8-1.2$

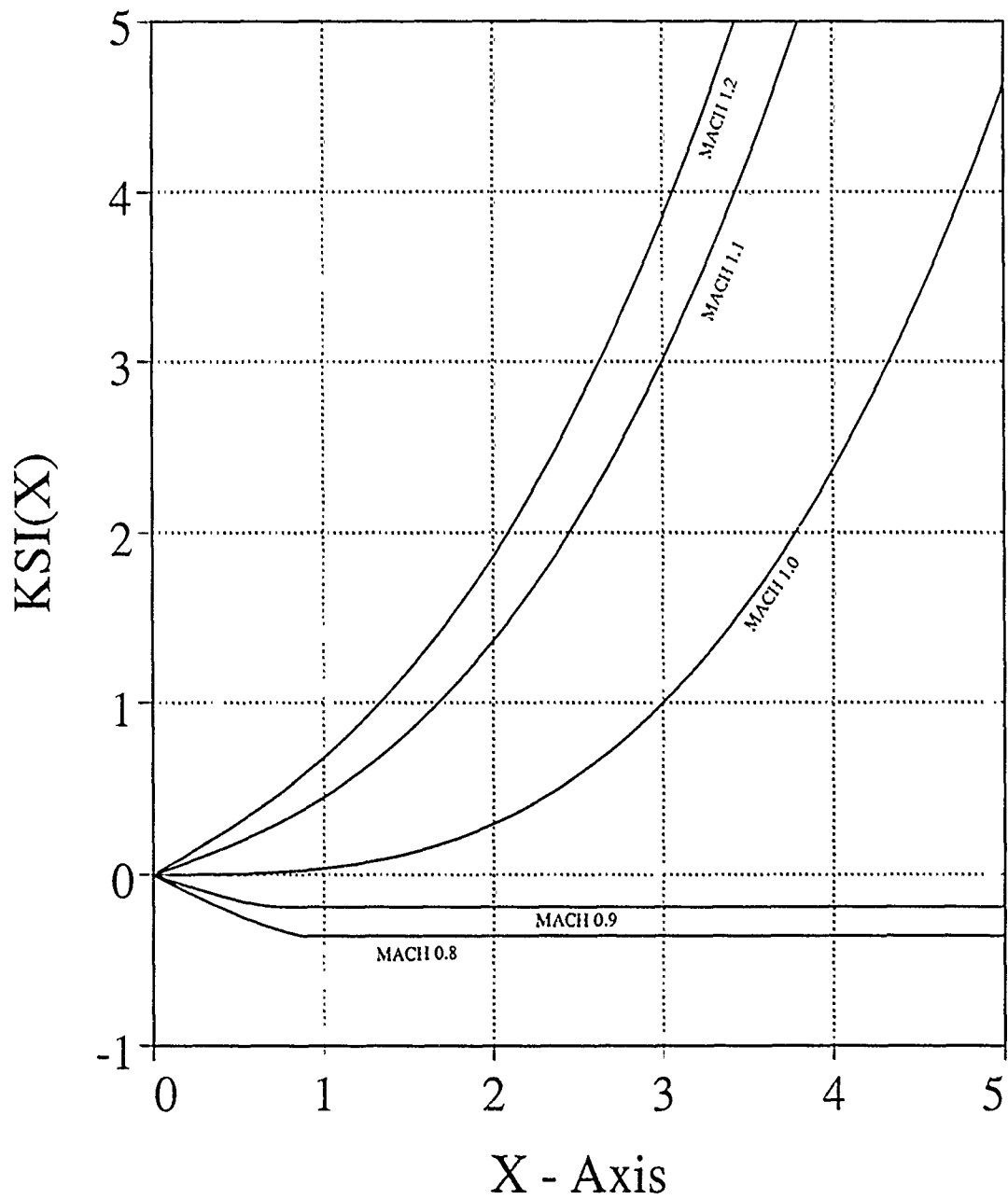


Figure 1. Numerical integration of eqns. 40 and 42.

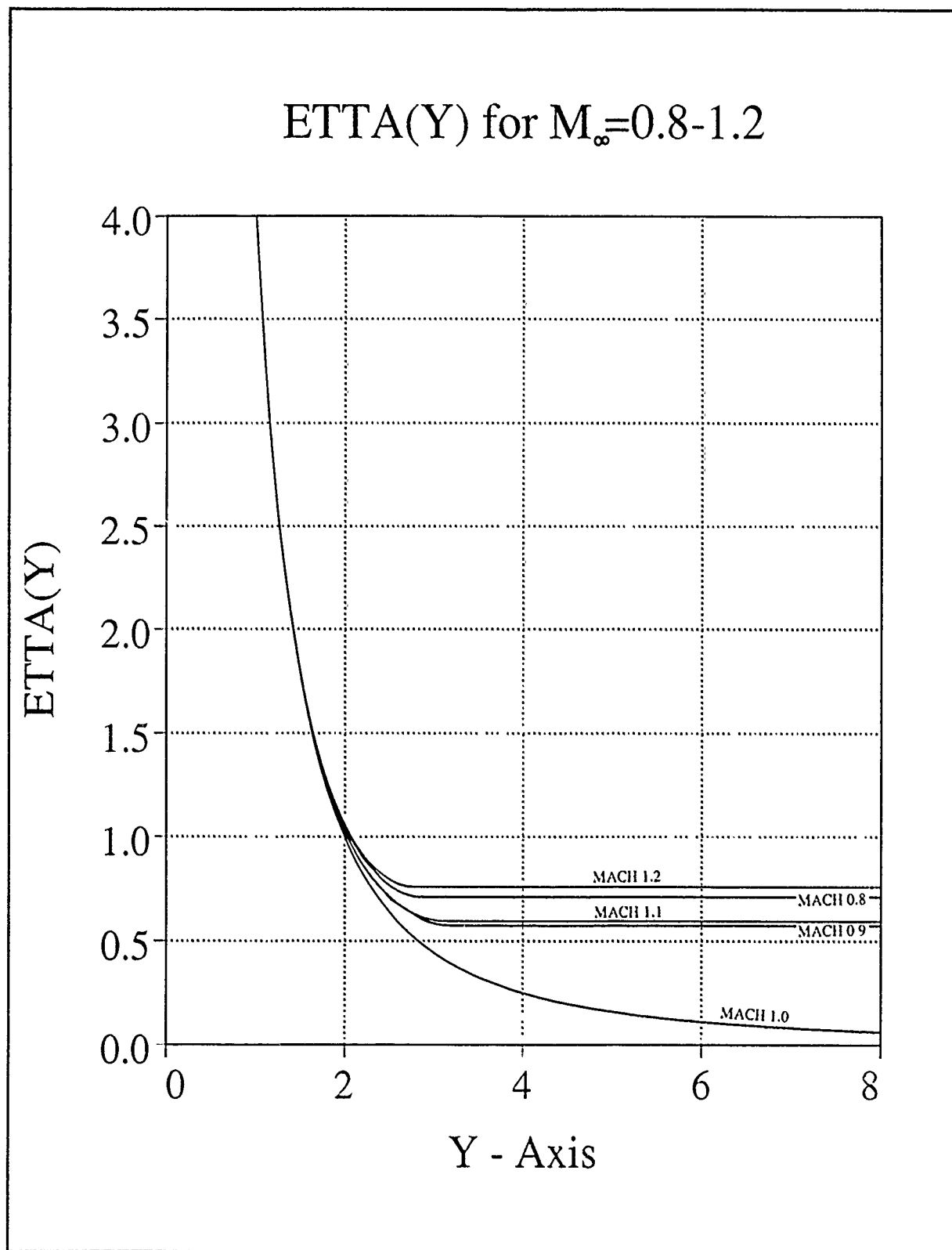


Figure 2. Numerical integration of eqns. 41 and 43.

$E(Y)$ vs. Y for $M_\infty=0.8-1.2$

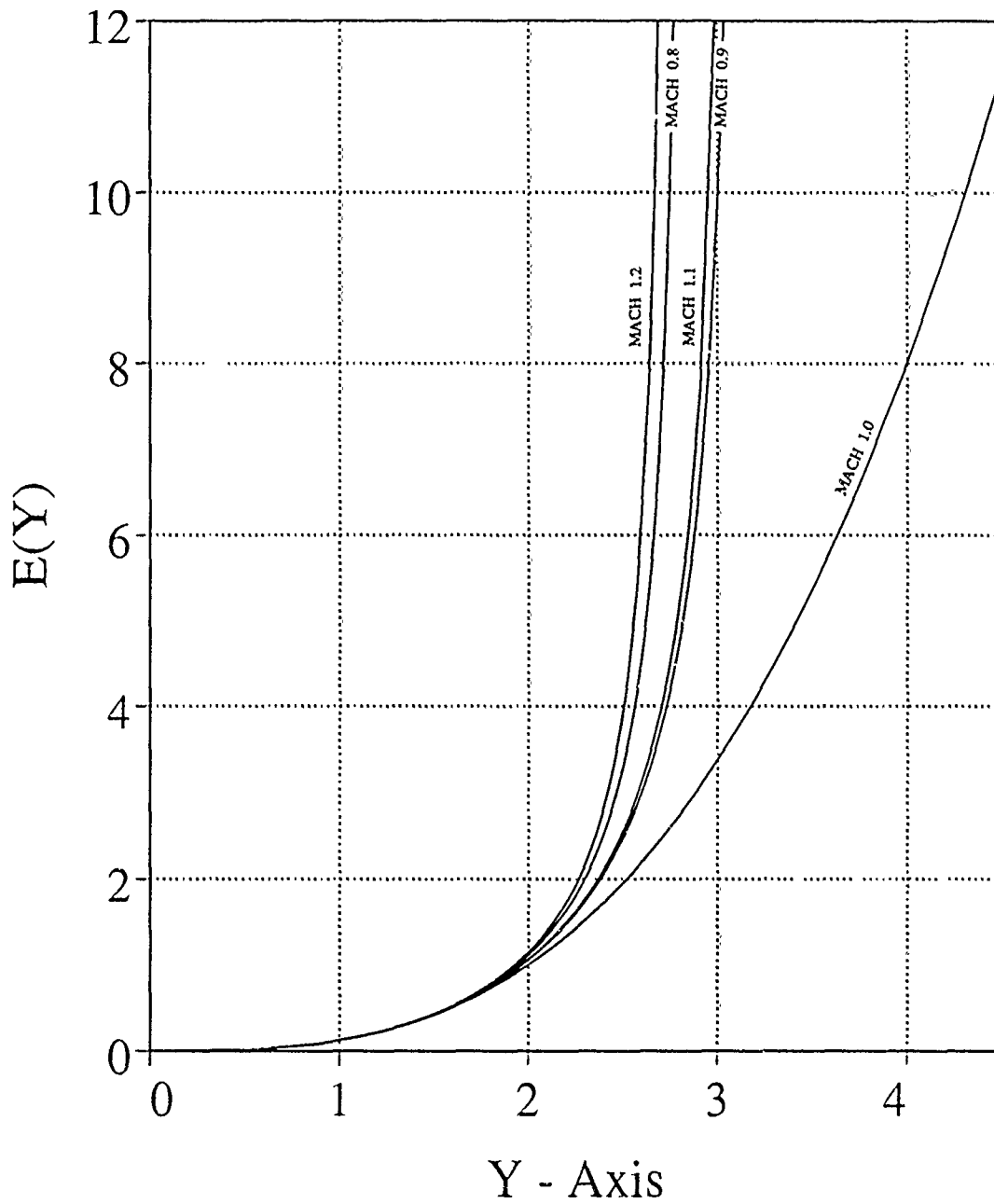


Figure 3. Numerical solution of $E(Y)$.

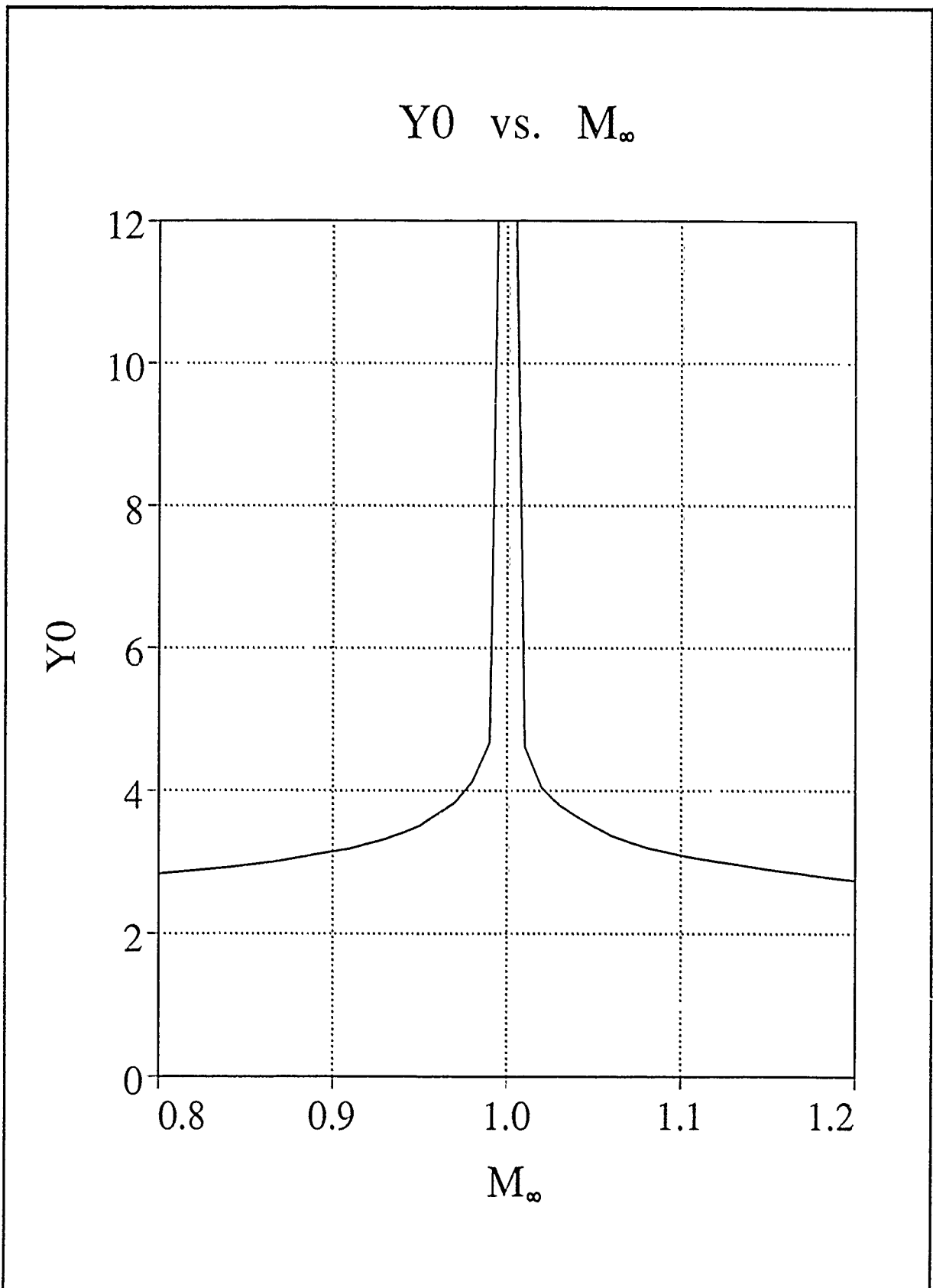


Figure 4. Equation 71.

$K(X)$ vs. X for $M_\infty=0.8-1.2$

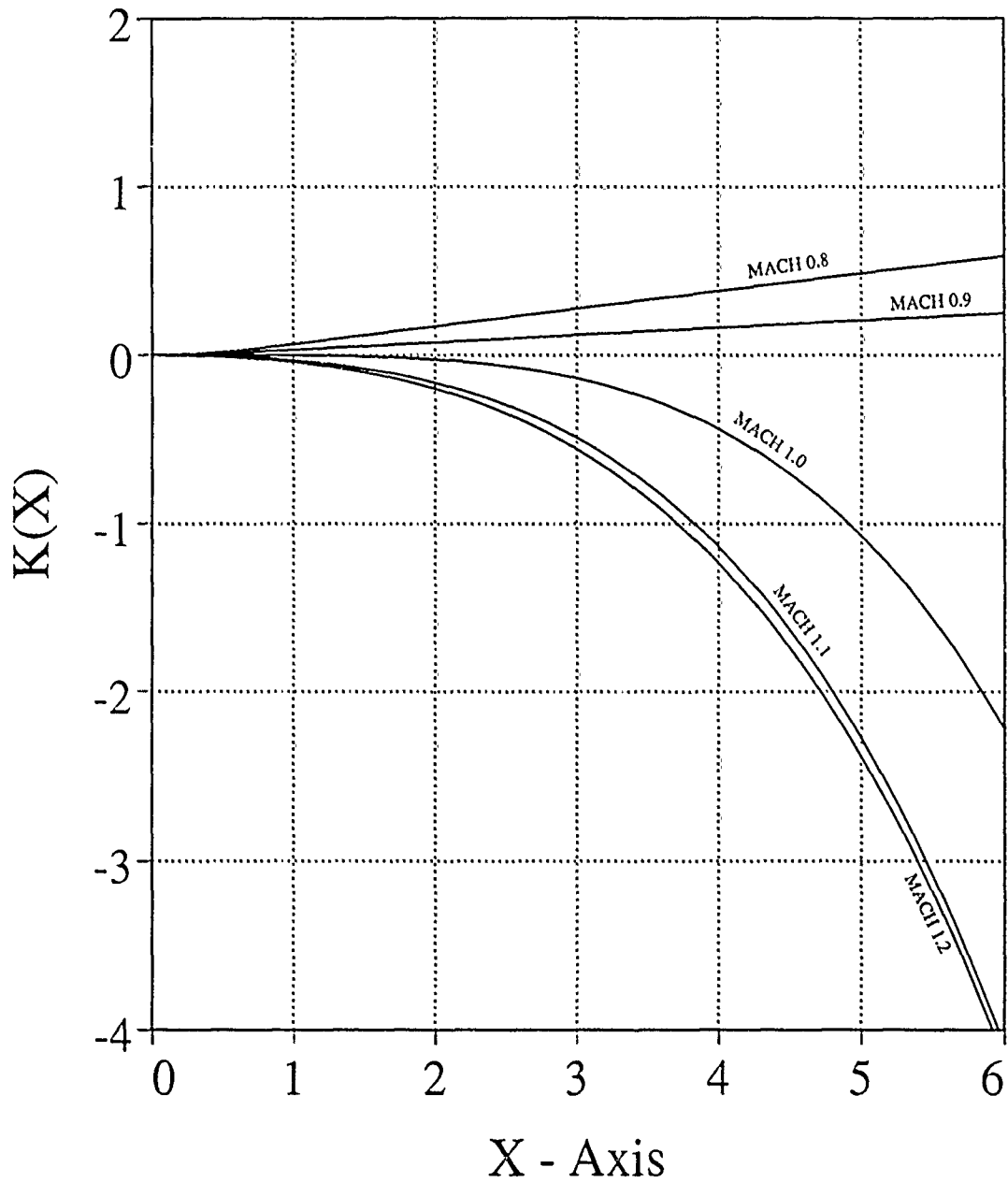


Figure 5. Numerical integration of eqn. 72.

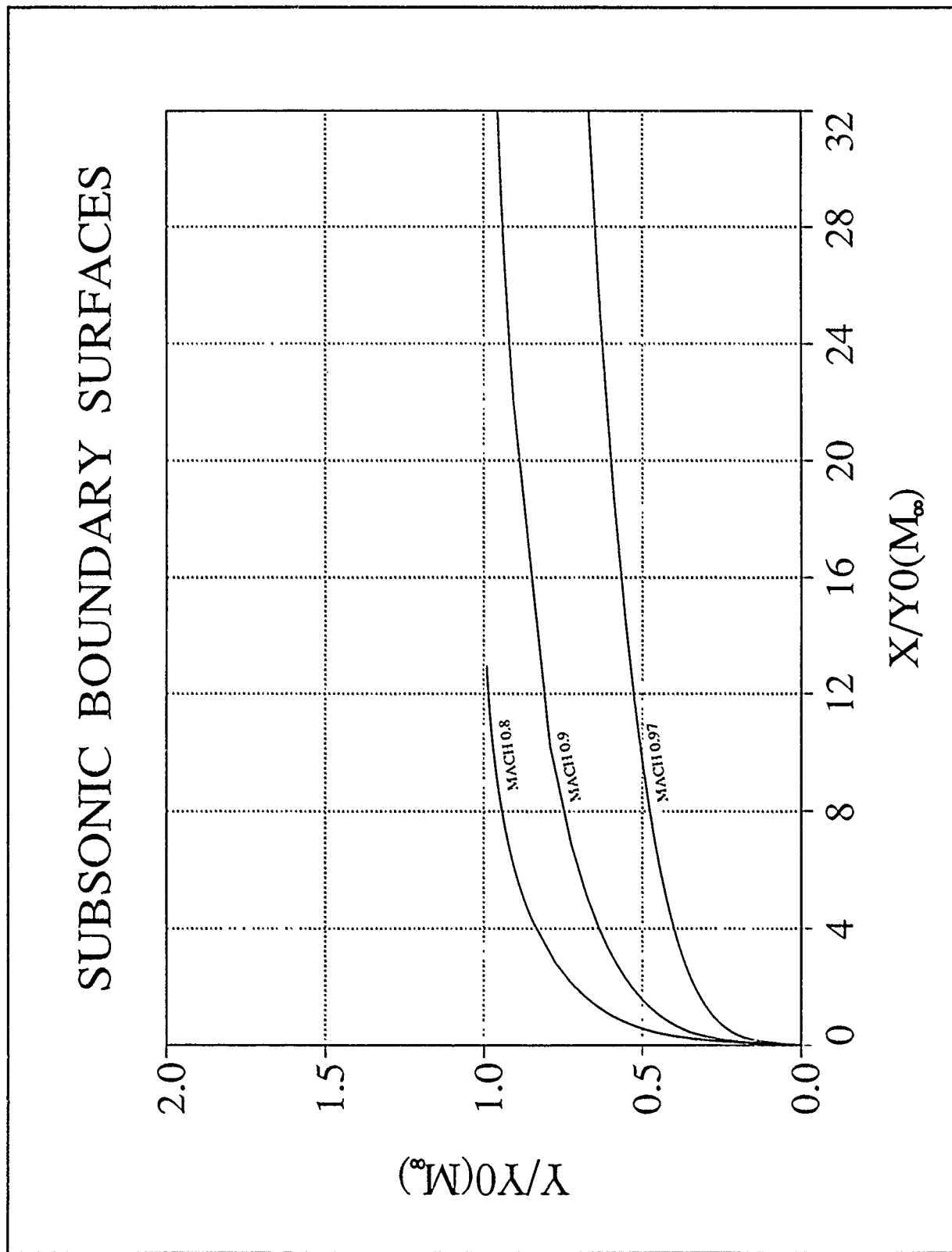


Figure 6. Numerical integration of eqn. 76.

SUBSONIC BOUNDARY SURFACES

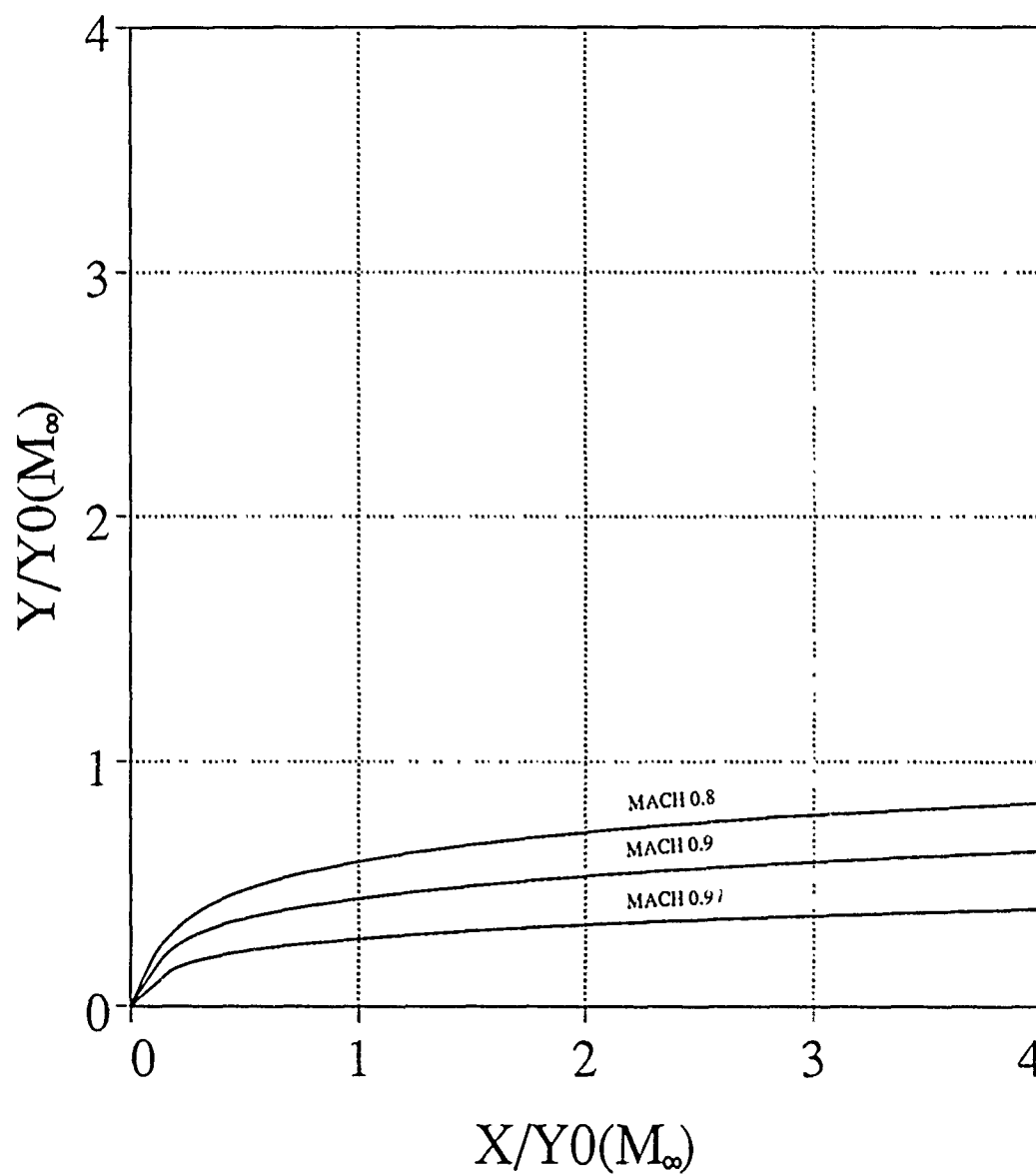


Figure 7. Subsonic boundary surfaces.

SUPERSONIC BOUNDARY SURFACES

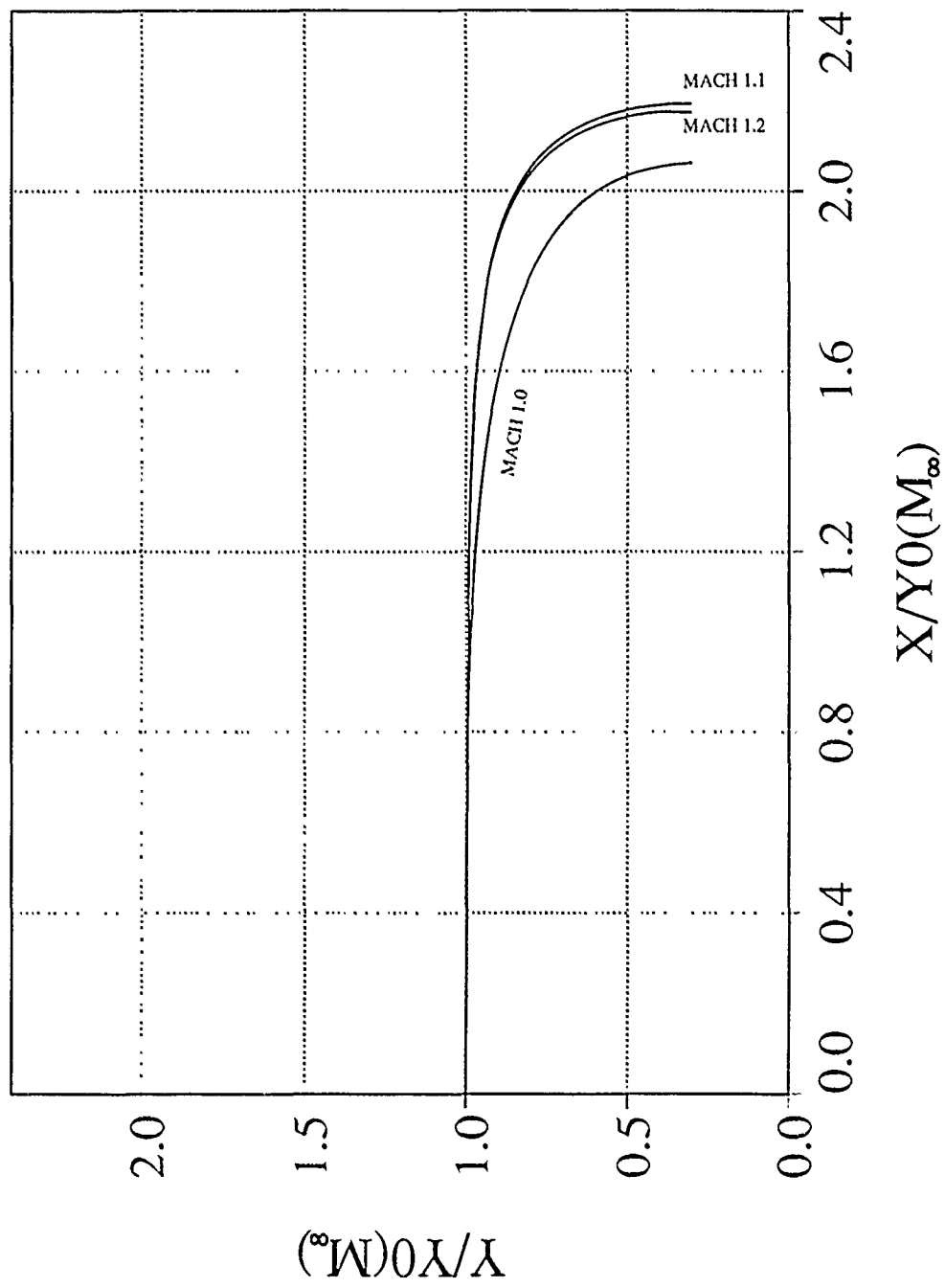


Figure 8. Numerical solution of eqn. 77.

Cp & local MACH FOR $M_\infty=1.0$

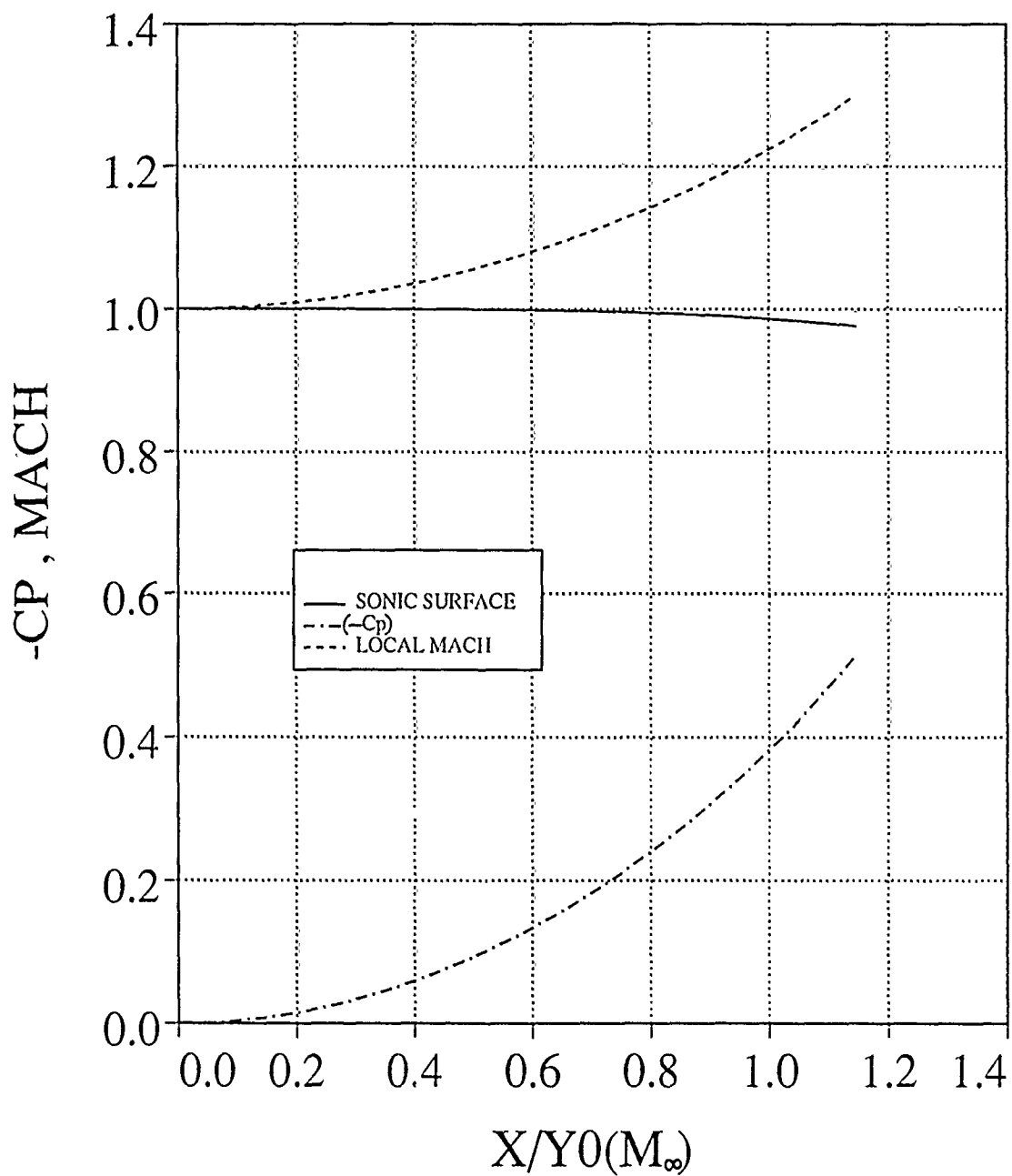


Figure 9. C_p and local Mach for $M_\infty=1.0$.

Cp & local MACH for $M_\infty=1.1$

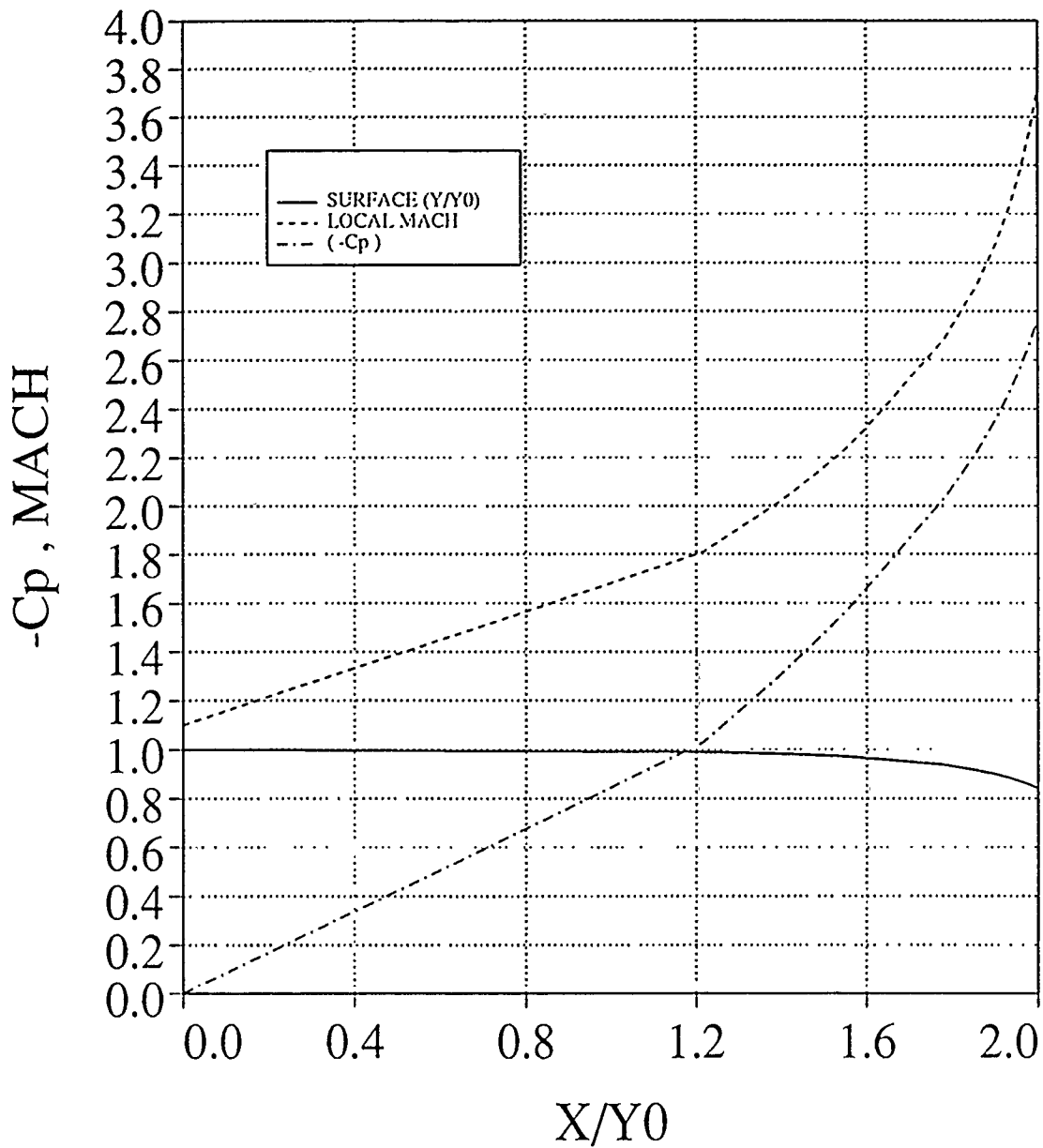


Figure 10. C_p and local Mach for $M_\infty=1.1$.

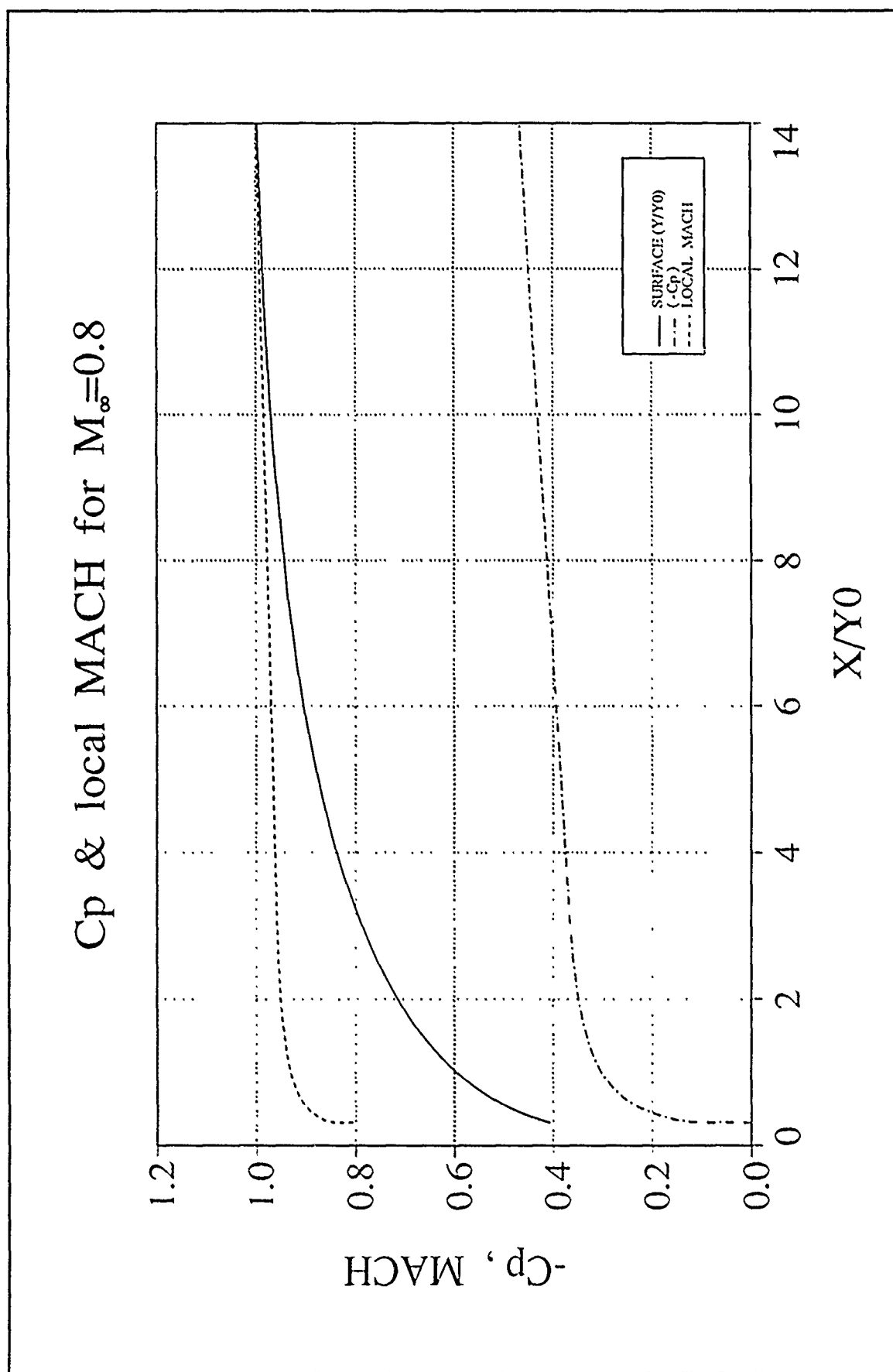


Figure 11. C_p and local Mach for $M_\infty=0.8$.

C_p & local MACH for $M_\infty=0.9$

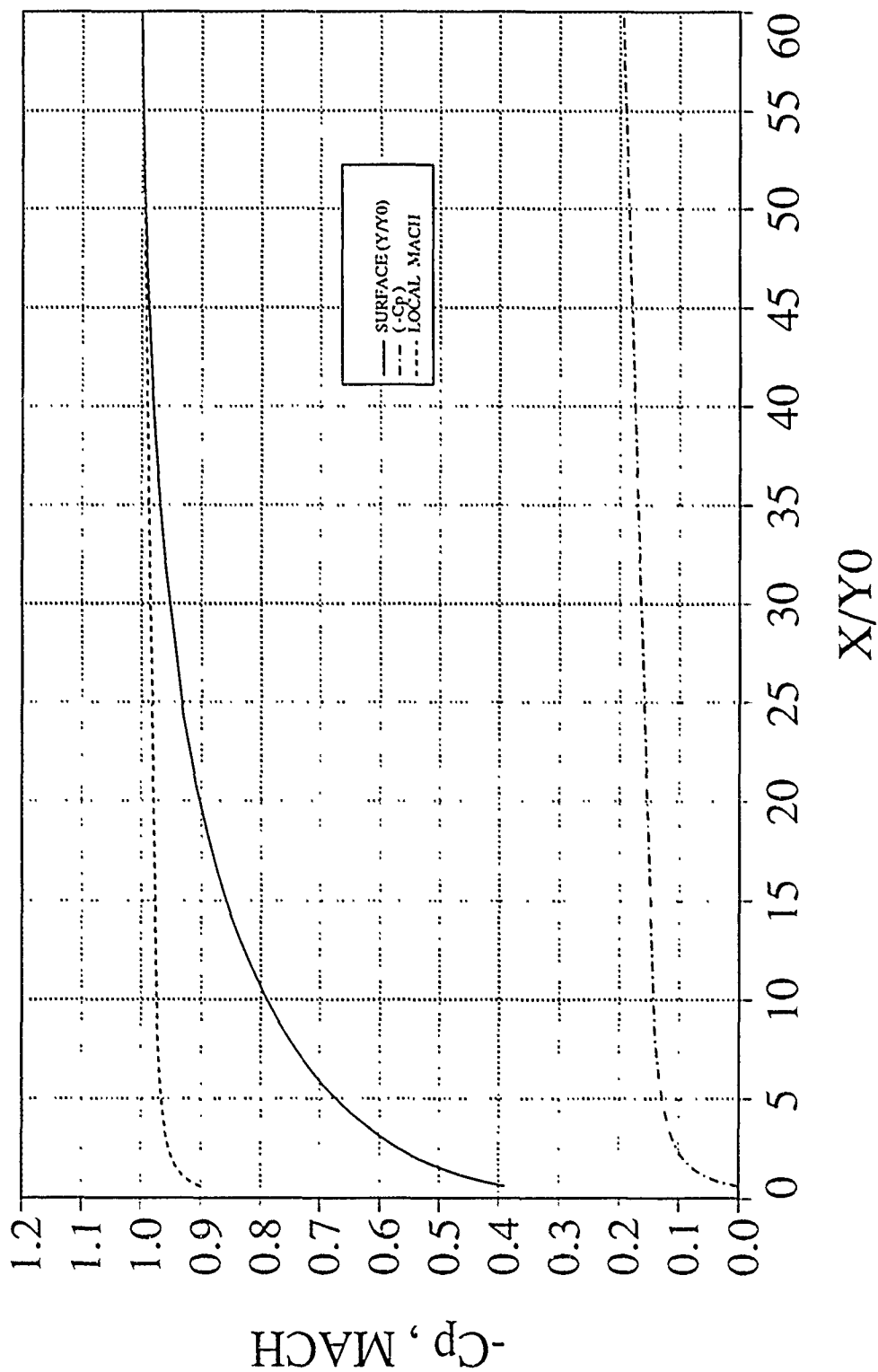


Figure 12. C_p and local Mach for $M_\infty=0.9$.

VELOCITY COLORED BY MACH NUMBER

CONTOUR LEVELS

0.00000
0.10000
0.20000
0.30000
0.40000
0.50000
0.60000
0.70000
0.80000
0.90000
1.00000
1.10000
1.20000
1.30000
1.40000
1.50000
1.60000
1.70000
1.80000
1.90000
2.00000
2.10000
2.20000
2.30000
2.40000
2.50000
2.60000
2.70000
2.80000
2.90000
3.00000

MACH 1.000
ALPHA 0.00 DEG
Re 9.00×10^6
TIME 27.
GRID 100x50

Figure 13. Velocity vectors for $M_\infty = 1.0$



Figure 14. Mach lines for $M_\infty=1.0$

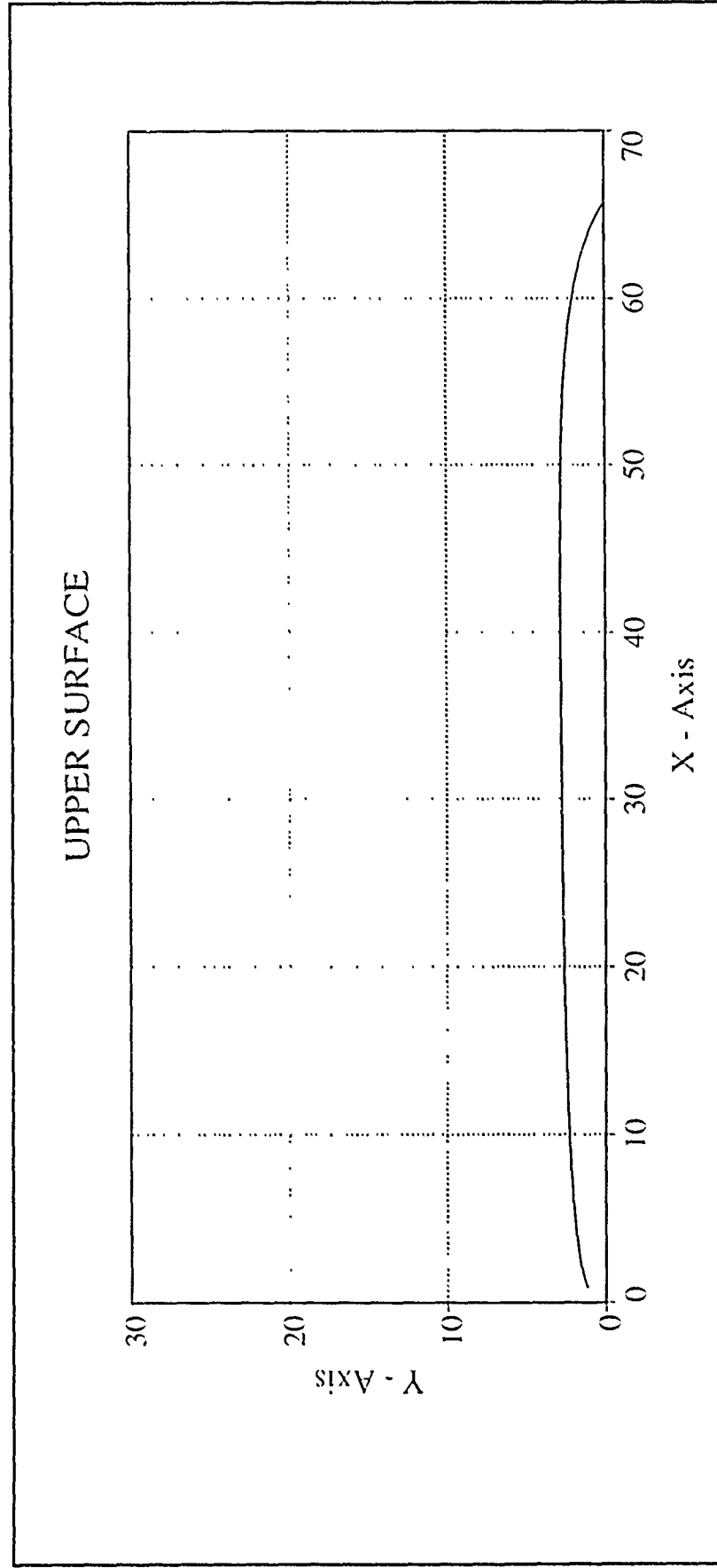


Figure 15. Upper transonic surface for $M_\infty=0.8$.

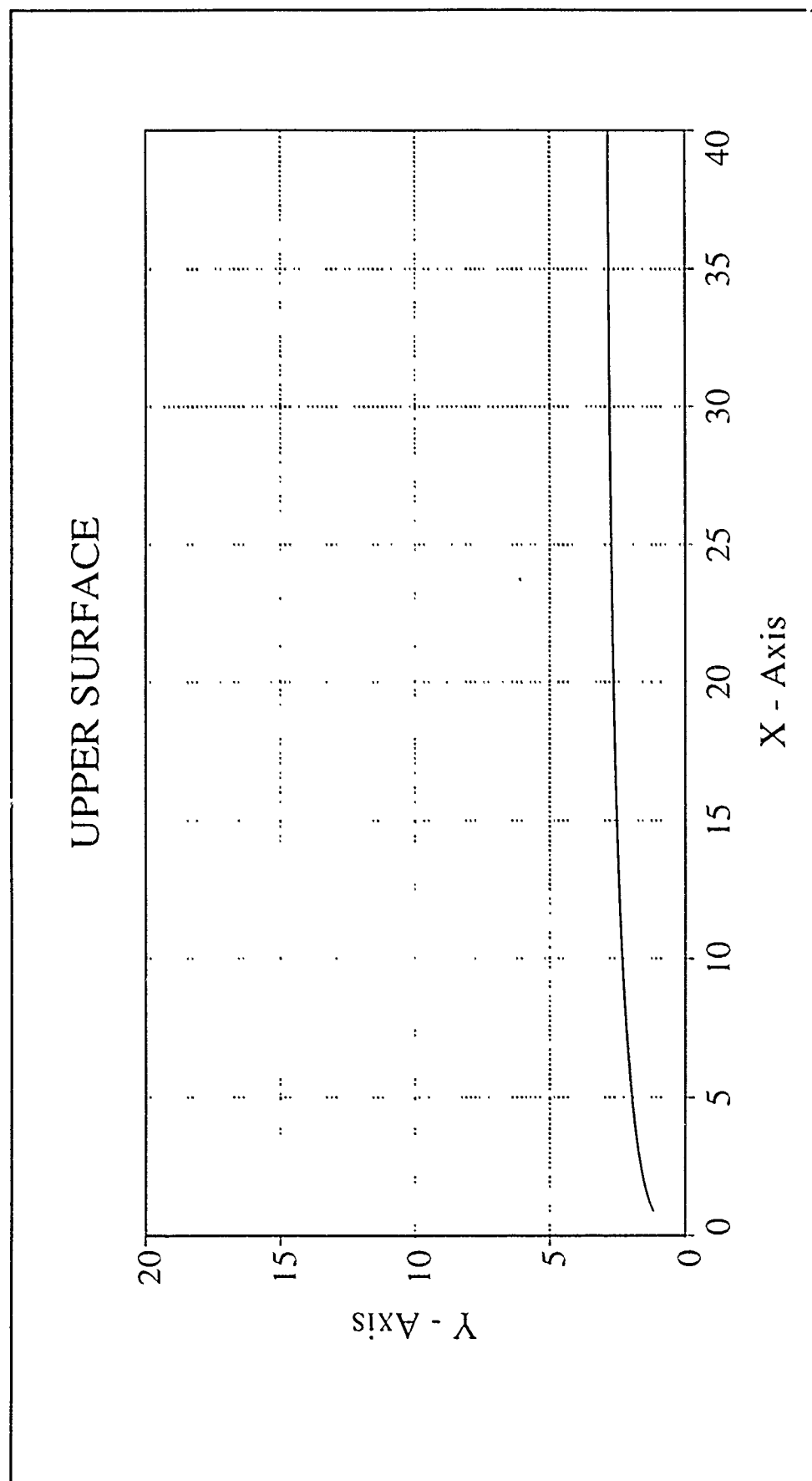


Figure 15a. Upper subsonic surface for $M_{\infty}=0.8$.

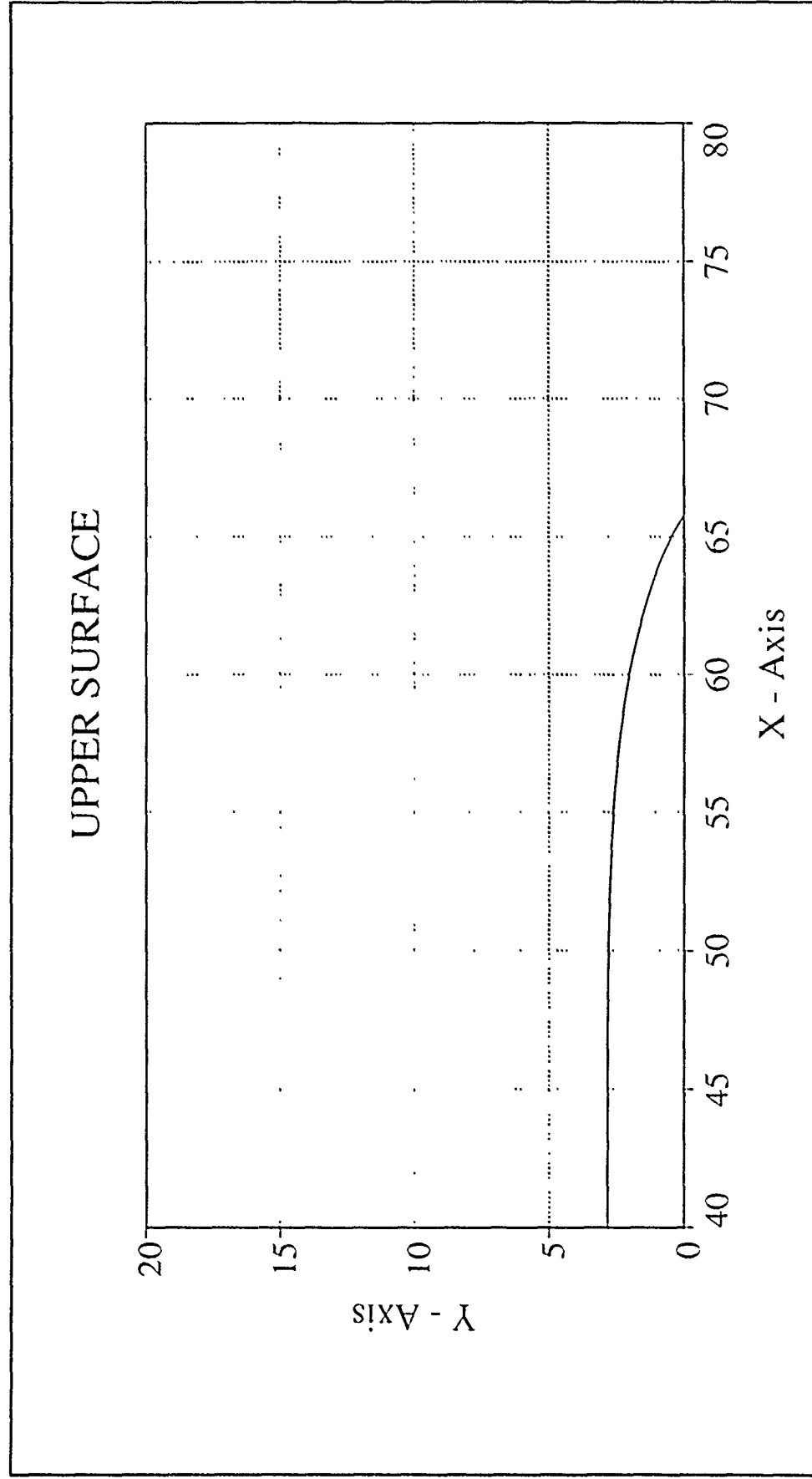


Figure 15b. Upper supersonic surface for $M_\infty = 1.0$.

KSI(X) FOR MACH 0.8 - 1.2

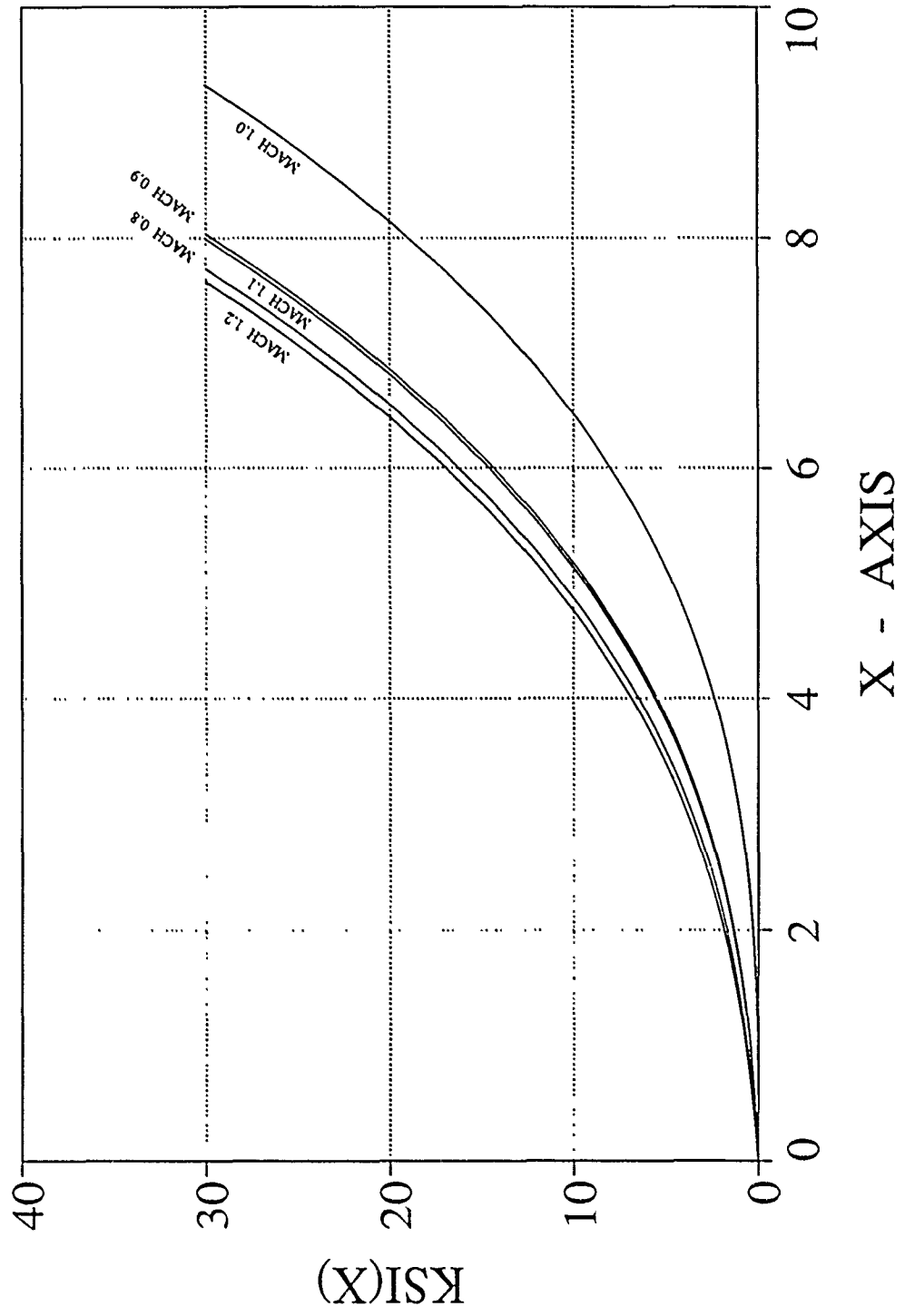


Figure 16. Numerical integration of eqn. 119.

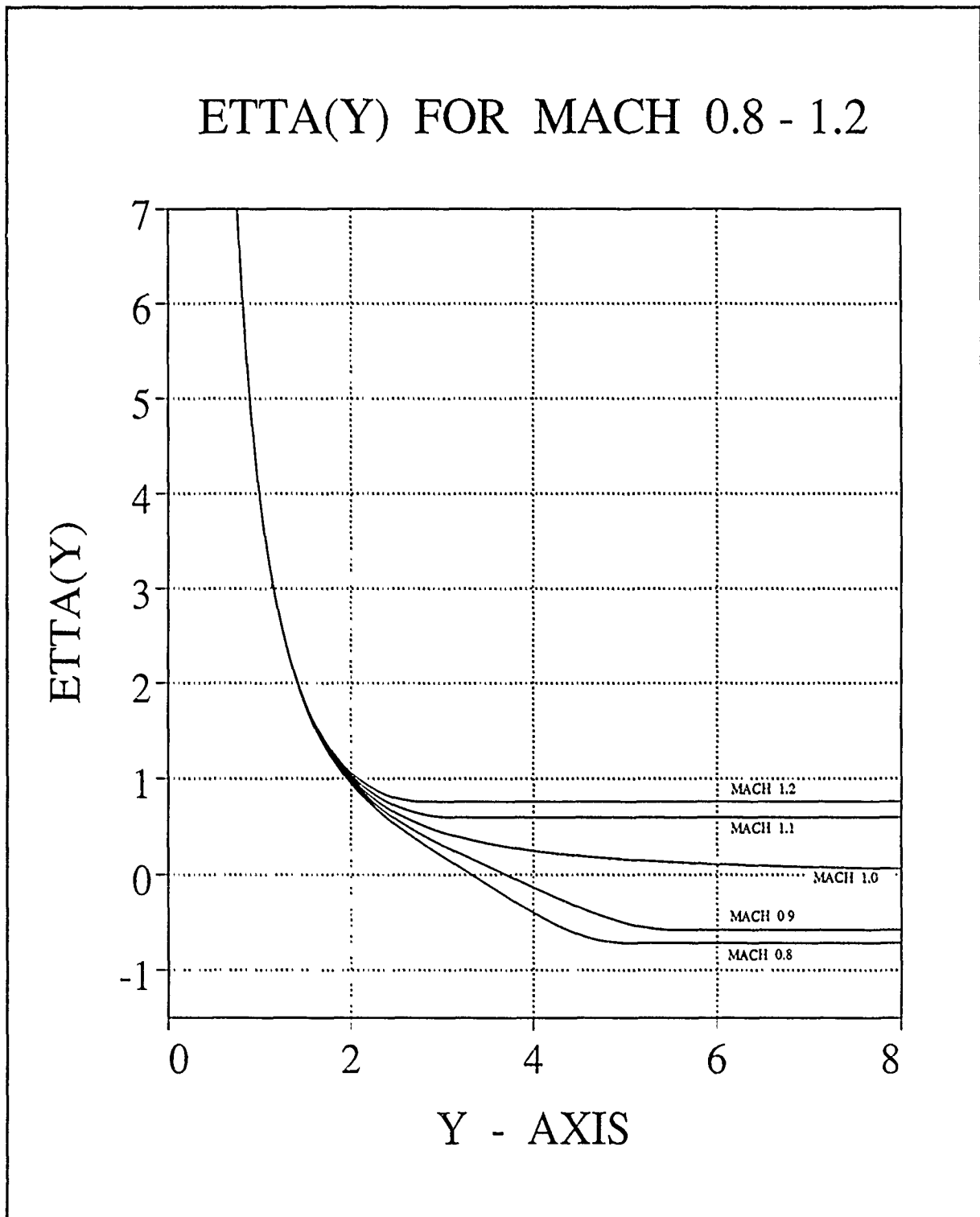


Figure 17. Numerical integration of eqn. 120.

BOUNDARY SURFACES for $M_\infty = 0.8-1.2$

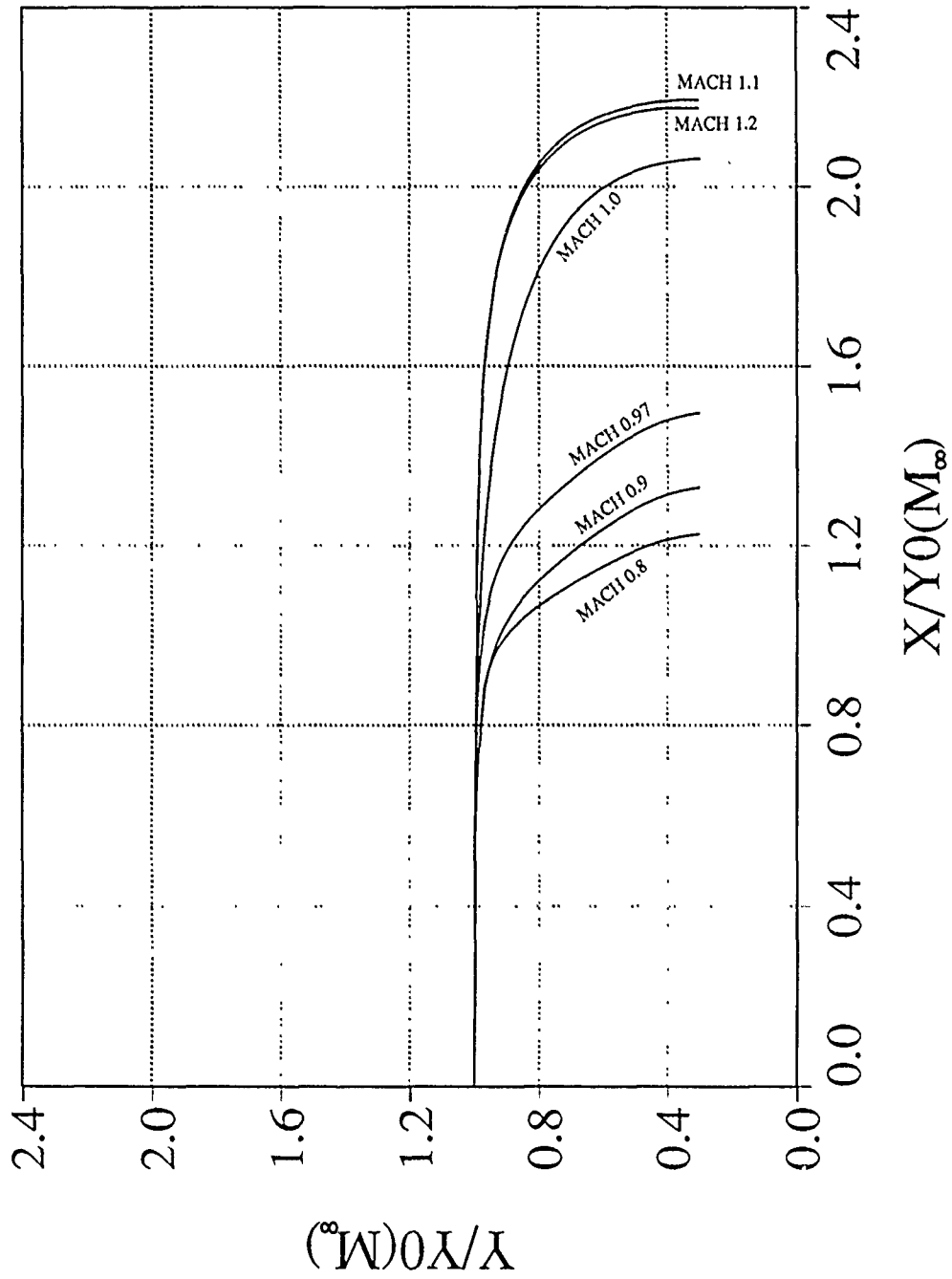


Figure 18. Numerical integration of eqn. 121.

CPsurface FOR $M_\infty=0.8$

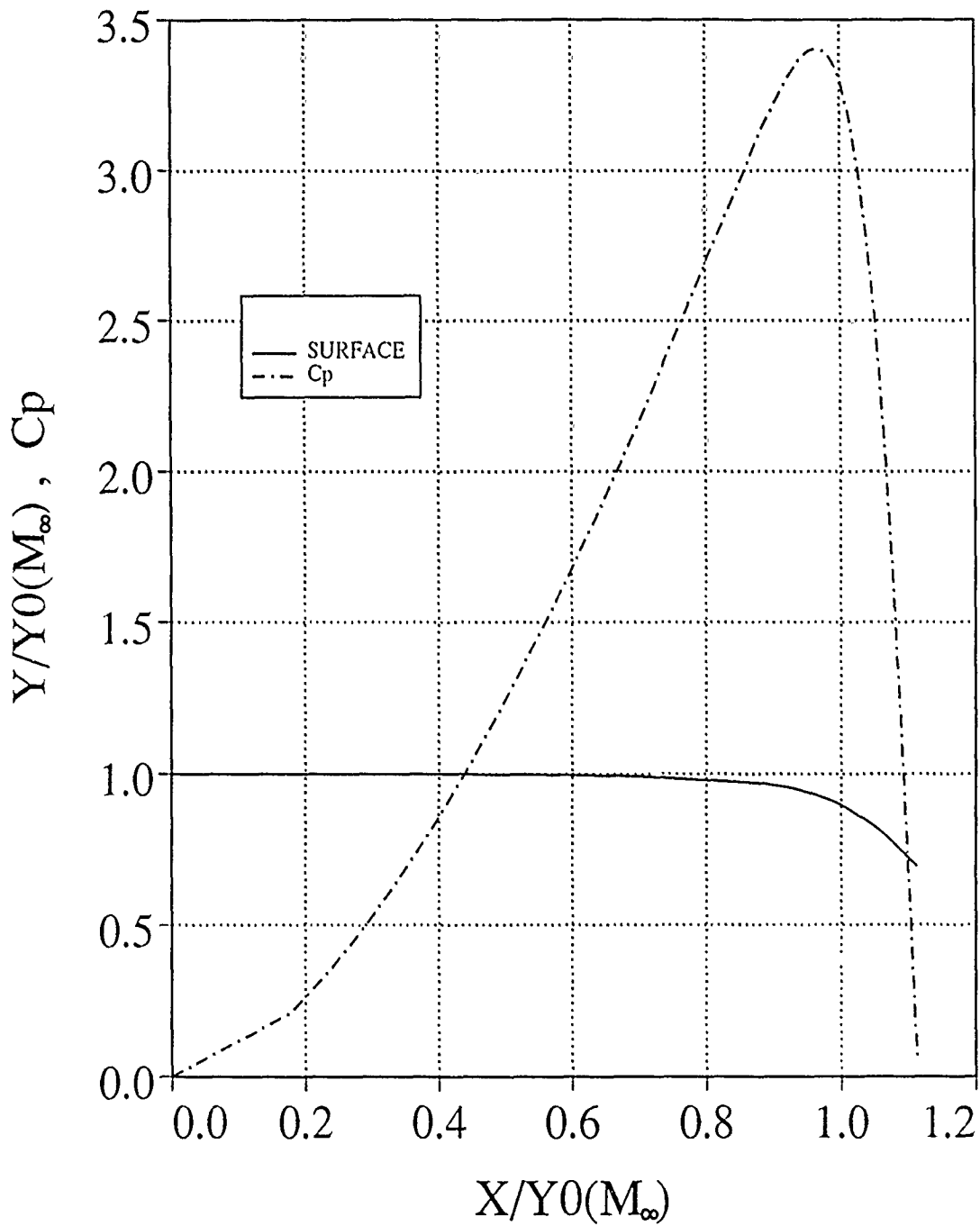


Figure 19. C_p for $M_\infty=0.8$.

INITIAL DISTRIBUTION LIST

		No. Copies
1.	Defense Technical Information Center Cameron Station Alexandria, VA 22304-6145	2
2.	Library, Code 52 Naval Postgraduate school Monterey, CA 93943-5002	2
3.	Chirman Department of Aeronautics, Code AA/Co Naval Postgraduate school Monterey, CA 93943-5000	1
4.	Prof. Oscar Biblarz Department of Aeronautics, Code AA/Bi Naval Postgraduate school Monterey, CA 93943-5000	2
5.	Prof. Garth Hobson Department of Aeronautics, Code AA/Hg Naval Postgraduate school Monterey, CA 93943-5000	1
6.	Prof. James V. Sanders Department of Weapons Engineering, Code PH/Sd Naval Postgraduate school Monterey, CA 93943-5000	1
7.	Dr. Craig Porter Naval Weapons Center, Code 3591 China Lake, CA 93555	1
8.	Mr. T. Boggs Naval Weapons Center, Code 389 China Lake, CA 93555	1
9.	Capt. Scotty Bates Naval Air Systems Command, Code AIR-540 Washington, DC 20361	1
10.	Maj. Aharon salama Department of Aeronautics, c/o Code AA/Bi Naval Postgraduate school Monterey, CA 93943-5000	3